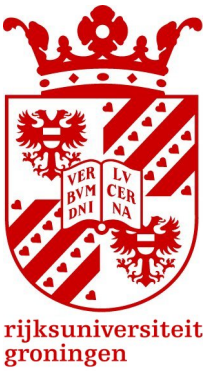

University of Groningen

Bachelor Thesis Project

Investigating the Utility of Topology Optimisation to Optimise the Mass and Thermal-Mechanical Properties of a Deeply Cooled Focal Plane Assembly

Author:
Matthias van Burg *(s4039297)*

Supervisors:
Prof. Dr. Ir. P. Onck
Prof. Dr. Ir. E. van der Giessen
Dr. Ing. R. Huisman
Ing. M. Eggens

June, 2025

Acknowledgements

I am grateful to all who have supported me throughout this research. First of all, I wish to express my gratitude to my supervisors Patrick Onck and Erik van der Giessen for showing interest, asking relevant questions and supporting me throughout the research. Secondly, my sincerest appreciation go out to Robert Huisman and Martin Eggens from SRON for the countless hours of help, advice and feedback they have given me and all the laughs we have shared. They have helped me steer this research in the right direction and provided ample guidance during the research. I am grateful to these individuals who have spent time and effort to aid me in this research.

Abstract

This research investigates the utility of topology optimisation to optimise a component in a deeply cooled focal plane assembly for its mass and thermal-mechanical properties. The novelty this research offers is the perspective on how to incorporate important system characteristics of an FPA in the topology optimisation process. The research concludes that to utilise topology optimisation for the thermal-mechanical optimisation of an FPA, the system characteristics must be identified and used to define the objective function and constraints in the optimisation process. The topology optimisation routine for an FPA must utilise a robust optimisation solver and an objective function which incorporates an internal energy for design connectivity.

The relevant system characteristics of an FPA were determined to be the effective thermal conductivity and capacity, the eigenfrequency and the von Mises stress. The thermal system characteristics were defined as FoM to assess the performance of the FPA whereas the eigenfrequency and von Mises stress were determined to be system constraints.

The objective functions in Solidworks were benchmarked for their performance and limitations. It was found that Solidworks offers only mechanical objective functions and no thermal optimisation is possible. The available objective functions considered maximising the stiffness, minimising displacement and minimising mass. These objective functions are not applicable to the optimisation of an FPA within the framework of this research.

A simplified FPA was optimised using the best stiffness to weight ratio objective function. The result yielded a 75% reduction in mass, 84.5% reduction in effective thermal conductivity and a 30% relative improvement in the effective thermal capacity.

Solidworks offers limited capabilities for the topology optimisation of an FPA. It is therefore suggested that the optimisation module in COMSOL Multiphysics is used for the topology optimisation of an FPA. Future research directions therefore includes, but is not limited to, investigating the topology optimisation routine in COMSOL, investigating the effect of optimisation solvers and identifying emergent properties for use as FoM.

List of Abbreviations

- FPA = Focal Plane Assembly
- SRON = Space Research Organisation Netherlands
- TES = Transition Edge Sensor
- X-IFU = X-ray Integral Field Unit
- KKT = Karush-Kuhn-Tucker
- FEM = Finite Element Model
- FEA= Finite Element Analysis
- CAD = Computer Aided Design
- OC = Optimality Criteria (method)
- MMA = Method of Moving Asymptotes
- BC = Boundary Conditions
- FoM = Figures of Merit
- DA= Detector Area
- TS = Thermal Strap

Contents

1 Introduction

In aerospace engineering, lightweight solutions are crucial to save money. The less mass one carries on a spacecraft, the less fuel one has to use to reach orbit. This is widely true for larger assemblies that serve a structural purpose. Some structures, mostly smaller sub-assemblies also thermally benefit from a decreased mass. These lightweight designs are optimised for a certain performance, usually with a lowest possible mass in mind. There are several methods to optimise a design: parameter, shape, size and topology optimisation. Shape and size optimisation are a form of parameter optimisation and work within a set of well defined parameters, such as be wall thickness, beam length and radii among others for size optimisation[1], whereas shape optimisation alters the shape of the geometry locally, where straight sections can turn into curved sections[1]. Parameter optimisation is usually defined by strict parameters such as loads and material choice, among others. Only topology optimisation is a different category as it changes the topology of the material itself; controlling material distribution within a domain[2].

Shape, size and parameter optimisation are limited in the range of design spaces they allow to explore, whereas topology optimisation allows for creative and unorthodox designs[3]. The first structural optimisation methods focused on the optimal, meaning lightest and cheapest, layout for trusses under a certain load[4]. This method considered the placement, length and orientation of structural beams to minimise the weight whilst maintaining structural integrity. About 80 years later, the idea of making the material distribution the design variable and use it in structural optimisation was proposed by Bendsoe and Kikuchi in 1988[2] and led to a cascade of research into the uses of topology optimisation for structural optimisation[5]. Although the first uses of topology optimisation were focussed on structural purposes, topology optimisation has recently also been used to optimise for thermal optimisation, or even a combination of both, as seen in [6] and [7]. Recently, truss layout optimisation has been researched using topology optimisation as a fundament, as showcased in [8]

This combination of mechanical and thermal properties is especially relevant in instruments used in space applications. One such example is the Focal Plane Assembly (FPA), which has stringent mechanical and thermal constraints imposed on it for the satellite sub assembly to perform optimally. This research focuses specifically on the FPA's produced by the Space Research Organisation Netherlands (SRON).

1.1 Introduction to FPAs

The Focal Plane Assembly is an integrated sub-assembly in satellites whose main purpose consists receiving and processing radiation from distant objects[9]. The assembly itself lies at the focal plane of the satellite's optics, where the radiation is incident on a detector array, key to the functioning of an FPA. The detectors are mounted on a support structure which also supports the readout circuit. The detector in an FPA consists of multiple pixels which can register the incident radiation, which can either be visible light, x-rays or infrared radiation, dependent on the mission. The type of radiation which is to be detected heavily influences the thermal-mechanical design of an FPA; considering this research focuses on deeply cooled FPA's, the missions which employ them will be the main inspiration for the design considerations of FPA's.

An example of an FPA is the one used in the Athena mission. This mission and its instrument will serve as the basis for FPA's in this research, meaning that the framework for optimising an FPA is built around the FPA used in the Athena mission. Other missions also contain FPA's, whose function is the same but have different system specifics; these will not be discussed. The FPA used as the fundament to understand the optimisation problem is part of the X-IFU spectrometer used to observe the hot universe [10][11]. The X-IFU FPA consists of three concentric stages: T2, being the outer structure wherein the other stages are mounted with a temperature of 2K. The T2 stage also contains a mu-metal shield which attenuates incoming magnetic fields. The T1 stage is an aluminum frame to which T2 and T0 are mounted using a suspension made of aramid chords. These aramid chords add stiffness to the whole assembly, but also thermally isolate the three stages from each other, allowing a relatively large temperature gradient between the three stages. The T1 stage is at a temperature of 0.3K. The T0 stage contains the housing of the detector array and readout electronics with a temperature of 0.05K. The T0 stage also contains a Niobium shield to further protect the detector and readout electronics. Niobium is a type II superconductor [**?**] and traps magnetic fluxes to prevent them from interfering with the sensitive electronics. The X-IFU FPA is shown in the figure below.

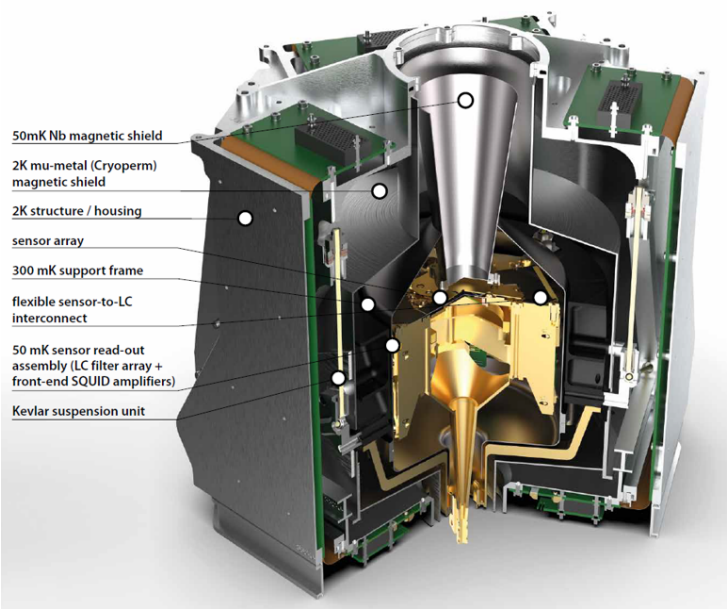

Figure 1: X-IFU FPA section view, as taken from [12].

The figure above shows the three concentric stages of an FPA and the respective temperatures. The inner layer, the T0 stage, contains the detector array, readout electronics and a connection to the cryocooler called the thermal strap. The cryocooler is responsible for cooling the inner stage by means of cooling a copper strap which is connected to the T0 stage. At the center of the T0 stage is the detector, more specifically a transition edge sensor (TES) [11]. The TES temperature is at 50mK and the material from which the TES is made is on the edge of being super- and normally conducting. Each incident photon will add heat to the detector and 'move' the energy of the electrons away from the superconducting edge, increasing the resistance[13]. This increase in resistance in turn influences the magnetic field produced in a wire connected to the TES. This change in magnetic field is subsequently interpreted to calculate the energy of the

incoming photon. These described processes make the TES sensitive to thermal fluctuations in the T0 housing and in the detector array, but also sensitive to outside magnetic fluxes. These sensitivities dictate the materials that can be employed for use in an FPA, as it must conduct heat well, but also not become superconducting at 50mK to be able to repel magnetic fields. For this reason, a high grade high purity copper is used in the X-IFU FPA [11] [14] as the bulk material of the T0 housing.

A close-up image of the TO housing is shown below.

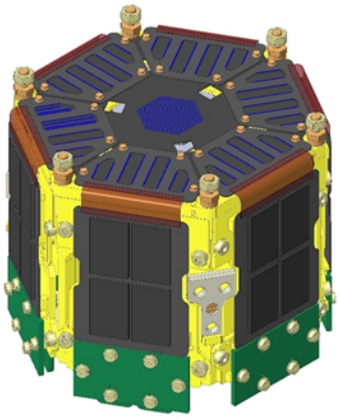

Figure 2: T0 stage of the X-IFU FPA, as taken from[11].

The figure above shows the T0 housing, where the yellow area is the copper material, the sides are clad with readout electronics and the top of the hexagonal structure holds the detector array in the centre. The copper housing is primarily made from bulk copper material and weighs 310 grams. Making this suspended T0 housing lighter will increase the resonant frequency of the structure and therefore allow for either shorter or thinner aramid chords, which will decrease the heat load from the different stages onto the T0 housing and its electronics. Decreasing the heat load is beneficial because then the detector array will have a lower operating temperature. There are several things to consider when making the structure lighter, such as the amount of material heat can flow through, away from the detector array, and the resonant frequency of the T0 housing. These are often conflicting interests, where reducing the mass, also reduces both thermal and mechanical aspects, such as the strength. This conflict in system characteristics introduces the optimisation problem for the FPA.

1.2 Problem Definition

The T0 housing made from copper is the component of interest in this research. Making the T0 housing lighter whilst preserving the ability to carry heat away from the detector and whilst keeping the structure stiff enough will improve the performance of the detector array. Going forward, further mentions of an FPA will not mean the whole assembly, but will only regard the copper T0 housing as the component to be optimised.

The goal of this research is to investigate how topology optimisation can be used to optim-

ise an FPA for its thermal and mechanical properties and to reduce its mass. To be able to assess the performance of an FPA, Figures of Merit (FoM) are introduced which describe system characteristics. The following research questions is therefore postulated:

> "How to utilise topology optimisation to optimise the mass and thermal-mechanical properties of a deeply cooled focal plane assembly by ascertaining a set of figures of merit?"

This research aims to answer this question by investigating different topology optimisation methods and manners of application, identifying what is relevant to optimise for in an FPA and how to quantify an FPA's performance. Lastly the previous two steps will be applied to a recreated FPA with the relevant details to verify and document the process. The purpose of documentation of the process is aimed at providing recommendations and further research to the scientists at SRON. This research is therefore focussed on the utility of topology optimisation for an FPA, and not on creating an optimised FPA in which all aspects are considered. General conclusions will be drawn on both fundamental and practical considerations for utilising topology optimisation for an FPA.

2 Optimisation Theory

To understand how to optimise an FPA, it is crucial to first discuss the process of general optimisation. The general theory behind optimisation will also serve as a basis for topology optimisation and its functioning. Additionally, the implementation of topology optimisation by several softwares is also of importance. This section therefore describes the mathematical background of relevant optimisation techniques and delves into the relevant topology optimisation softwares and their functioning.

2.1 General Optimisation

The goal of optimisation is to arrive at a minimum or maximum of a function. The function in question is called the objective function $J(\mathbf{x})$. This objective function can either be constrained or unconstrained, depending on if there are constraints imposed on the values of parameters within the objective function. Lastly, the objective function and its respective constraints can be considered linear or non-linear, considering that topology optimisation is a non-linear optimisation problem, this section will only deal with non-linear optimisation.

Considering the objective function $J(\mathbf{x})$ with its respective design variable $\mathbf{x}$, a general mathematical formulation of a non-linear and constrained optimisation problem is defined as[15]:

$$\begin{aligned} \text{minimise} \quad & J(\mathbf{x}) \\ \text{subject to} \quad & g_i(\mathbf{x}) + a_i \geq 0 \quad \text{i} = 1,...,\text{k}, \\ & g_i(\mathbf{x}) - a_i \leq 0 \quad \text{i} = \text{k}+1,...,\text{m}, \\ & g_i(\mathbf{x}) - a_i = 0 \quad \text{i} = \text{m}+1,...,\text{p} \end{aligned}$$

This formulation states that the objective function is to be minimised subject to a set of constraints, which are either equality or inequality constraints. These constraints restrict the design space wherein an optimum can be found. In an application, these constraints can be the resonant frequency of a system, or the maximum allowable von Mises stress. Important to note here is that the constraints are also functions of the design variable.

Constrained problems are usually solved by introducing the Lagrangian equation, which combines the objective function and the constraints. This is done, because the value of the constraints influence the 'location' of the optimum [15]. The Lagrangian is given by:

$$\mathcal{L}(\mathbf{x}, \lambda) = J(\mathbf{x}) - \sum_{i=1}^{p} \lambda_i [g_i(\mathbf{x}) - a_i] \tag{1}$$

Where λ_i indicate the Lagrange multipliers. In non-linear constrained optimisation, the optimum is therefore not only determined by the objective function, but by a linear combination of the objective function and the constraints, as dictated by the Lagrangian. In order to find an optimum, there a set of necessary conditions that must be met, called the Karush-Kuhn-Tucker (KKT) conditions [15]. It is important to note that these conditions necessitate the existence of an optimum, but do not necessitate the optimum to be the global optimum. Consider the value

of the design variable $\mathbf{x}^*$ to be a local maximum or minimum of our objective function $J(\mathbf{x})$. The KKT conditions then impose the following:

$$g_i(\mathbf{x}^*) - a_i \text{ is feasible, i = 1,...,p} \tag{2}$$

$$\nabla J(\mathbf{x}^*) - \sum_{i=1}^{p} \lambda_i^* \nabla g_i(\mathbf{x}^*) = \mathbf{0} \tag{3}$$

$$\lambda_i^* [g_i(\mathbf{x}^*) - a_i] = 0 \text{ i = 1,...,m} \tag{4}$$

$$\lambda_i^* \geq 0 \text{ i=1,...,m} \tag{5}$$

$$\lambda_i^* \text{ unrestricted for i = m+1,...,p} \tag{6}$$

Note that the above conditions consider different values of i, where some conditions only apply to inequality constraints, as indicated by i = 1,...,m.

The above conditions are the necessary conditions for $\mathbf{x}^*$ to be an optimum. Condition 1 found in equation 2 states that at the optimum, the constraint is feasible, ensuring that the constraints are met. The second condition in equation 3 states that the gradient of the Lagrangian must be 0, implying the stationarity of the optimum, so that a change in the design variable will not simultaneously improve the objective function and the constraint. The third condition in equation 4 is called the complementary slackness condition, which essentially implies that either the Lagrange multiplier is zero, or that the constraint is 0. This condition ensures that constraints which are non zero; put practically: constraints which are far from being at their given limit, do not participate in the optimisation. Constraints which are not at their given limit are called inactive constraints, and do not directly influence the optimisation; as soon as the constraint is at, or within a predefined tolerance to, its given limit, it becomes active and will influence the optimum. The last two conditions dictate the sign of the Lagrange multipliers for (in)equality constraints. It is essentially equation 3 and 2 which must be solved for, to find $\mathbf{x}^*$ and λ^*. These values are solved for and updated iteratively until the problem converges to a solution.

The optimisation problems can be solved in different manners, which will be called optimisation solvers or solvers, in which the most common ones are the Optimality Criteria Method (OC)[16] and the Method of Moving Asymptotes (MMA) [17]. Understanding the means by which these solvers 'steer' towards a solution is crucial in explaining its behaviour in an applied setting. Important in the following sections is the distinction between optimisation solvers and topology optimisation methods: the first is a mathematical method to solve a general optimisation problem, whereas the latter is a method on how the material in topology optimisation is mathematically described.

2.1.1 Optimality Criteria Method

Both OC and MMA are inspired by the KKT conditions described in equations 2 through 6. It is especially the second condition that serves as a basis for these solvers. The optimality criteria method is a heuristic approach based on the second condition of the KKT conditions[16]. Firstly, the Lagrangian function is created from the objective function as seen in equation 1 and the stationarity of the Lagrangian is imposed as the optimality criteria, in other words, if

equation 3 is true within tolerance, the solution has converged to an optimum. The gradient of the Lagrangian has two values that must be calculated and updated at each iteration: the design variable $\mathbf{x}$ and the Lagrange multiplier λ_i. The Lagrange multipliers are calculated using a bisection method to converge to a value each iteration whereas the design variables are determined using the optimality condition [5] as given by:

$$B_e = \pm \frac{\frac{\delta J}{\delta \mathbf{x}}}{\lambda \frac{\delta g}{\delta \mathbf{x}}} \tag{7}$$

The sign in the above ratio can be either positive or negative depending on the behaviour of the objective function and the constraints. If the ratio is equal to 1, the gradient of the objective function and the product of the Lagrange multiplier with the gradient of the constraint are equal and thus, stationarity of the Lagrangian has been achieved. Note that the above equation is valid for an objective function with a single constraint $g(\mathbf{x})$. If the optimisation problem contains multiple constraints, the above version of the optimality criteria can no longer be used and a generalised optimality criteria method (GOC) is proposed and used[16]. The GOC defines the optimality criteria now as a sum of the constraints[16]:

$$B_e = -\frac{\sum_{i=0}^{m} \lambda_i \frac{\delta g_i}{\delta \mathbf{x}}}{\frac{\delta J}{\delta \mathbf{x}}} \tag{8}$$

In the above equation, the constraints are put into the numerator to avoid dividing by zero, as the Lagrange multipliers can also be 0 depending on the active or inactive nature of the constraint, as explained in section 2.1. These optimality criteria are used as indicators in another equation to determine the value of the design variable in the next iteration.

A method proposed by Bendsoe and Kikuchi [2] for a specific use case employs a heuristic approach to iteratively converge to a solution, depending on the value of the optimality criteria. In this heuristic approach, two factors are introduced, called the positive move limit m, and the numeral damping coefficient η. These parameters are usually set to 0.2 and 0.5 respectively for the specific use case and influence the speed at which the Optimality Criteria can converge. The move limit indicates how 'big' the jump can be, avoiding large jumps in solutions to avoid overshooting.

The main issue with the OC is its lack of ability to handle multiple constraints well. Within the most popular use case, the design variable is updated independently of the other design variables. This updating independence implies that each design variable is individually updated based on local optimality criteria [3]. This ensures that a unique solution to the Lagrange multiplier can be found for each iteration. When however, a new constraint is added, the Lagrangian stationary condition as seen in equation 3 expands. In an extended formulation, the design variables and Lagrange multipliers become coupled through multiple constraints and have to be solved for simultaneously [16], leading to an increase in computational complexity. This issue is resolved in the GOC defined in equation 8, in which the authors of [16] worked around satisfying the KKT conditions in every step, avoiding the iterative process to find the Lagrange Multipliers. Another example where the OC has been improved to handle multiple constraints can be found in [18].

2.1.2 Method of Moving Asymptotes

The MMA is, alongside OC, a popular optimisation solver. Conceived in 1987 by Svanberg [19], it was intended for structural optimisation where strictly convex sub-problems where created each iteration so that they can easily be solved. MMA, similar to OC, also uses the derivative of the objective function in its formulation to converge to a solution. As mentioned, the optimisation routine exists of two layers of problems to solve: the first layer approximates the objective and constraint functions by defining it strictly as a convex problem as follows[19]:

$$J_i^{(k)}(\mathbf{x}) = r_I^{(k)} + \sum_{j=0}^{n} \left(\frac{p_{ij}^{(k)}}{U_j^{(k)} - x_j} + \frac{q_{ij}^{(k)}}{x_j - L_j^{(k)}} \right) \tag{9}$$

In which $J_i^{(k)}$ is the iterative approximation of the objective function, but is also interchangeable with the constraint functions g_i as seen in 2.1. The r_i is the residual, U_j and L_j are the moving asymptotes and p_{ij} and q_{ij} are placeholder variables for functions of the derivative of the function J_i or g_i. Important to note is that the values of U_j and L_j are chosen such that:

$$L_j^{(k)} < x_j^{(k)} < U_j^{(k)} \tag{10}$$

As the asymptotes move closer to the design variable value $x_j^{(k)}$, the approximating function becomes a better representation of the original problem. The aforementioned variables are to be updated each iteration; their value is determined by the second layer, which creates the Lagrangian from the function as seen in equation 9 and subsequently tries to minimise the Lagrangian with respect to the design variable. It does this by calculating the first and second derivative of the Lagrangian, which as a consequence shows that the first derivative of the Lagrangian is only increasing in x_j. One can then conclude there is a unique solution to x_j which only depends on the Lagrange multipliers. This unique solution inherently decouples the design variable x_j from all Lagrange multipliers and itself, and as a consequence allows for the separate and independent solving of the Lagrange multipliers for the initial problem. Each x_j will have their own sub-problem to solve, which involves imposing the Lagrangian stationarity condition on the separated x_j Lagrangian.

The MMA solver is a powerful optimisation tool because it allows for the separation of the design variables into separate sub-problems to reduce complexity. Additionally, it inherently allows for multiple constraints because these are simply added in the second layer in which individual x_j are solved, and therefore pose no grave issue in computational complexity. Despite the clear strength of MMA in dealing with a large number of design variables and constraints, there are also issues with regards to the fact that the MMA employs a heuristic approach to adjusting the asymptotes U_j and L_j. This fact is illustrated in the original paper by Svanberg,, in which it states that the process can tend to oscillate or stagnate depending on the values of the asymptotes [19]. This asterisk is irrelevant to this research, as most softwares with the MMA solver automatically select these asymptotes.

2.2 Topology Optimisation

Topology optimisation is an optimisation method that uses the material distribution as its design variable to come to an optimal design considering a certain objective function and a set of respective constraints [2] [3]. In topology optimisation, the design to be optimised is first discretised into a Finite Element Model (FEM), which it uses to perform a Finite Element Analysis (FEA) to compute such things as von Mises stress, strain energy or displacement. This calculation is preceded by the introduction of important system parameters, such as material properties and imposed boundary conditions needed to solve the FEA. In the FEA, it also calculates the first value of the objective function. The most common objective function, stemming from the structural engineering historical relevance [2], is the compliance. Constraints are usually a volume constraint, maximum allowable stress, displacement or eigenfrequency. The objective functions and constraints can also be extended to thermal problems, as illustrated by [7].

The topology optimisation problems are formulated in a similar fashion as seen in 2.1.Additionally they are solved in a similar fashion by means of introduction of the Lagrangian. Important to note, is that not all methods to solve an optimisation problem introduce the Lagrangian, but the ones relevant to the scope of this research do. Introduced with the Lagrangian, are the derivatives of the objective function and the constraints, these are also crucial in understanding where the optimum lies. Understanding where the solution lies is, in part, done by understanding how the Lagrangian moves with infinitesimal changes in the design variable; called a sensitivity analysis [15]. This sensitivity analysis is done every iteration, where the gradient of the objective functions and constraints as a function of the design variable are calculated. This analysis indicates how sensitive the 'optimal' solution and the Lagrangian are to changes in the design variable and can tell something about the 'direction' the optimisation needs to proceed in. The above has described the general process of how topology optimisation converges to an 'optimal' solution and is reiterated in the figure below, where the general process of a topology optimisation routine is shown.

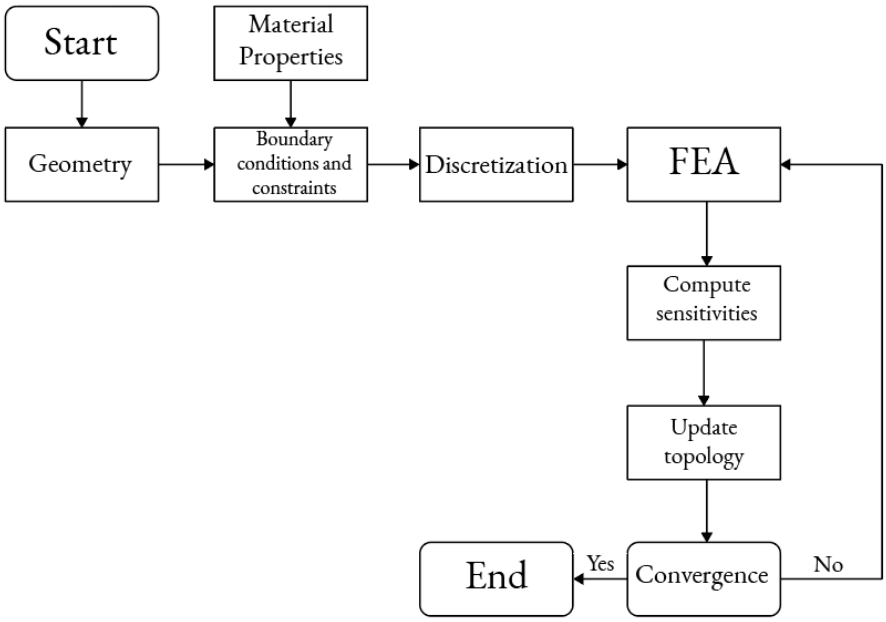

Figure 3: Showing the general process of a topology optimisation routine.

There are several methods that can be employed to yield an optimised design; these are divided into two groups[5]: Trial and error schemes, and gradient based. Within the second group are yet again distinctive methods for topology optimisation of which density based and the level set approach are the most prominent [5]. All methods have their own benefits and drawbacks, such as computational cost or based on what problem they are applied to; this research however, will not discuss the differences of these methods. For a complete overview of these different methods, the reader is referred to [5].

2.2.1 Solid Isotropic Material with Penalization

The most commonly used method to describe the material distribution in topology optimisation is the Solid Isotropic Material with Penalization method (SIMP), conceived in 1989 by Bendsøe [20]. This method assigns a density variable ρ_e to each finite element e in the finite element model. The density can range from 0, being void, to 1, being solid material. To avoid numerical issues with 0 density elements, a ρ_{min} is defined, so that an element can exhibit a density:

$$0 < \rho_{min} \leq \rho_e \leq 1 \tag{11}$$

Since each element can exhibit a different density value, their properties change too. The Young's modulus of the elements are scaled with the element density and an applied penalty as follows:

$$E(\rho_e) = \rho_e^p E_0 \tag{12}$$

Where E_0 is the isotropic value of the Young's modulus of the assigned material and p is a penalty factor, usually 3. The penalty factor makes it so that elements with a lower density contribute less to the global stiffness; hence the name, solid isotropic material with penalization.

The Young's modulus is directly related to the stiffness of a system, consequently, changing the Young's modulus element wise, will change the global stiffness tensor. The stiffness tensor of an element is scaled according to the density and original element stiffness tensor $K_e^{(0)}$ as such [21] [5],

$$\mathbf{K_e} = (\rho_{min} + \rho_e^p(1 - \rho_{min}))\mathbf{K_e^{(0)}} \tag{13}$$

Where the global stiffness tensor will be the geometric sum of these element wise stiffness tensors. Solving the topology optimisation problem will find the distribution of element densities such that a given objective function is minimised or maximised.

Within the SIMP method, and within topology optimisation in general, the most common objective function for which to solve is the stiffness of a structure, or rather, its compliance under a given load. In the optimisation, the compliance is minimised, which is equivalent to maximising the stiffness. The compliance is defined by the element densities, the displacement and global stiffness tensors. The compliance is the sum of these properties over all elements, and is given by[21]:

$$C(\rho) = \sum_e^N (\rho_e^p)\mathbf{u_e^T}\mathbf{K_e}\mathbf{u_e} \tag{14}$$

Where N is the total number of elements, $\mathbf{u_e}$ and $\mathbf{K_e}$ are defined as the displacement tensor and stiffness tensor, respectively, of the element e. The above equation is similar to the equation used in finite element models to calculate the total strain energy. Equation 14 calculates the total strain energy by summing over all individual strain energies of the elements in the FEM. This means that the total strain energy and stiffness of a system are intrinsically linked. Instead of the factor $\frac{1}{2}$, the density penalty is introduced, where elements with low density, contribute less to the total strain energy than elements with high density. This penalty ensures that intermediate densities are not preferred, but densities of 0 and 1 are. With only an objective function however, the optimisation problem is unconstrained, so a volume constraint is usually applied to restrict the 'amount of material' the optimisation can remove. Essentially, this constraint dictates the weight of the final design, but is described in terms of volume due to the finite element nature of the problem. This constraint, called the volume fraction. is usually added to make the optimisation a constrained problem and is given by:

$$\frac{V(\rho)}{V_m} - V_f = 0 \tag{15}$$

Where the V_m is the maximum volume as seen in the unoptimised model and V_f is the volume fraction defined in the optimisation. Important to note is that the volume $V(\rho)$ is defined as [22]:

$$V(\rho) = \sum_{e=1}^N \rho_e v_e \tag{16}$$

Where v_e is the element volume. Lastly, the finite element model must satisfy force-stiffness equilibrium conditions as given by:

$$\mathbf{KU} = \mathbf{F} \tag{17}$$

The above culminates to the most common topology optimisation problem, where compliance is minimised with a given volume constraint, governed by force-stiffness equilibrium conditions and a range of element densities. The optimisation problem definition is similar to that seen in

section 2.1, however, now tailored to topology optimisation with constraints on the volume and element density.

$$\begin{aligned} \text{minimise} \quad & C(\rho) = \sum_{e}^{N} (\rho_e^p) \mathbf{u_e^T K_e u_e} \\ \text{subject to} \quad & \frac{V(\rho)}{V_m} - V_f \leq 0 \\ & \mathbf{KU} = \mathbf{F} \\ & 0 < \rho_{\min} \leq \rho_e \leq 1 \end{aligned}$$

As mentioned in section 2.2, in gradient based methods, which SIMP is a part of, the sensitivities of the objective function and constraint are to be calculated with respect to the design variable. This sensitivity analysis is useful in assessing the impact of the changing the design variable on the 'optimal' solution. For the most common case of compliance and volume constraint, these are given by:

$$\frac{dC}{d\rho_e} = -p(\rho_e)^{p-1} \mathbf{u_e^T K_e^{(0)} u_e} \tag{18}$$

The sensitivity of the compliance is calculated for each element, to accurately asses the impact of individual changes in element density on the compliance. The sensitivity of the volume is more straightforward, as it is defined as a function of element density and element volume, the gradient is constant:

$$\frac{V(\rho)}{\rho_e} = v_e \tag{19}$$

The constant gradient leading to a constant term as a constraint, defined as $\frac{v_e}{V_m}$.

The SIMP formulation is especially powerful in combination with the OC method, as there is no additional calculation that is required for the sensitivities of the objective function or the volume constraint. The sensitivity of the compliance is plainly the strain energy as calculated in the static calculation. The OC method combined with the SIMP formulation therefore employs the optimality criteria B_e which is defined as [3]:

$$B_e = \frac{-p(\rho_e)^{p-1} \mathbf{u_e^T K_e^{(0)} u_e}}{\lambda_e v_e} \tag{20}$$

The above equation and the heuristic updating scheme defined in section 2.1.1 have as a consequence that elements with a strain energy larger than the product $\lambda_e v_e$ will subsequently see their densities increased, in other words, the numerator is greater than the denominator. In the case where the denominator is larger than the numerator, the element density will decrease, within reasonable bounds as to not violate the density constraints.

As mentioned in section 2.1.1, the OC method is built for handling a single Lagrange multiplier, which in this case is the one belonging to the volume constraint. The Lagrange multiplier and the element density can be calculated independently, making the SIMP formulation and the OC method a robust combination. The problem arises when multiple constraints are introduced and multiple Lagrange multipliers exist. Solving for multiple Lagrange multipliers is feasible, but if the element density and Lagrange multiplier become coupled through a global system

characteristic, the OC method encounters difficulties. The SIMP formulation in combination with the MMA method has been performed before as seen in [7] but has been less described in literature.

2.3 Applying Topology Optimisation

The theory as described above has been long implemented in multiple softwares since its first conception in 1989. The extent of the abilities of the softwares differs, where some are more customizable than others. In this section, the softwares considered for applying the topology optimisation will be discussed with key characteristics, differences between softwares and their limitations. The considered softwares are Creo Parametrics, COMSOL and Solidworks, and will be discussed in respective order.

2.3.1 Creo Parametric

Creo Parametric is a CAD software which was readily available for use in this research. Although a powerful designing tool, its topology optimisation capabilities are limited. The software allows for an extensive parameter optimisation, where one can customise the details of the optimisation to get the desired result, but this use case is however not considered. Creo Parametrics topology optimisation abilities are within the 'Generative Design' option in the software. A key note is however that generative design is not topology optimisation. Both methods function with specified constraints, which can be on stress, displacement or even symmetries. Whilst the outputs of both methods may look similar, the key difference is that generative design will explore the whole design space, beginning with a set of requirements and calculating all possible design that satisfy these requirements [23], whereas topology optimisation will converge to a design. Generative design has also been created to incorporate manufacturing constraints such as additive manufacturing or sintering. It is nonetheless important to note that topology optimisation is the foundation of generative design.

The generative design capabilities are limited in Creo Parametric. The design goal is singular and specified as 'maximise stiffness by minimising strain energy' with only a volume constraint that can be applied together with manufacturing constraints. In the software, there is no consideration of maximum allowable von Mises stress, resonant frequency or nodal displacement. Generative design is a powerful tool that can in essence consider more than topology optimisation alone can, but the capabilities within Creo Parametric are limited.

Lastly, because generative design within Creo Parametric is a more exploratory algorithm, where all feasible designs are considered, it is much more taxing on one's hardware, adding another limiting factor to the software. The meshing of the created geometry is especially heavy on the CPU whereas the optimisation process taxes the GPU heavily; the set-up used in this project does not have sufficient capabilities to be able to properly handle these tasks.

2.3.2 COMSOL Multiphysics

COMSOL Multiphysics is also a powerful tool allowing multiple physical disciplines to be combined, such as thermal and mechanical, within the same model. Next to being a multiphysics software, its optimisation capabilities are also widespread, as it is able to perform size, shape and topology optimisation as well as parameter estimation. The software also has extensive documentation on the mathematical background of its modules.

COMSOL, opposite to Creo Parametric, allows almost full customization of the optimisation process. The user can apply a density model to the created CAD geometry, in which almost all relevant settings can be changed, such as the density attribution method, which can be different from the aforementioned SIMP method. Secondly, within the optimisation itself, different optimisation solver methods, such as MMA, among others, can be employed to solve the optimisation problem. One is able to choose the solver method most fit to the problem at hand, which can be relevant as seen in [17] and [5]. Lastly, which is arguably the most potent function of COMSOL, is the ability to define the objective function. Where other softwares, like Creo Parametric, have preset objective function which optimise for a single measurable objective, COMSOL has the ability to define an objective function. One is for example able to optimise for the thermal gradient across a selected area on the CAD geometry. Additionally, one can also create a combination, linear or non linear, a ratio or otherwise, of different system properties, such as the total strain energy and the effective thermal conductivity to optimise for a specific set of system characteristics. Similarly, the applied constraints can also be customised to this extent. This customisability allows for a specific optimisation of certain system characteristics, making COMSOL a powerful tool for optimisation considering thermal and mechanical properties.

What COMSOL, unlike Creo Parametric, does not consider is the potential manufacturability of a design. There are no settings which dictate, for example, that symmetry must be retained in the part, or a minimum size a structural member can have. In other softwares, these are settings which can easily be identified and used, whereas in COMSOL, these must be created by the user; where one can specify an area to be kept, or a radius to be a specific value. Because there is less focus on these applied aspects of topology optimisation, achieving some manufacturing goals can be difficult.

As a practical consideration, optimisation in COMSOL ensures that there is no exporting of the geometry needed from one software to the other to perform a design verification. The exporting of the geometry from one software to the other can cause issues and a possible loss in geometrical detail, this is further touched upon in section 5.4.

2.3.3 Solidworks

Solidworks is a software focused on mechanical designing, in which fluid flow and thermal simulations can also be done, albeit in separate simulations. There is also a topology optimisation study in Solidworks with a range of objective functions and design and manufacturing constraints available. Unlike Creo Parametric, these manufacturing constraints are not for additive manufacturing, but are more focused on symmetry and de-molding possibilities.

As mentioned, there are several objective functions available in Solidworks, these are:

1. Best stiffness to weight ratio
2. Minimise maximum displacement
3. Minimise mass

Unlike in COMSOL, there is no infinite freedom for which system characteristic the software optimises, nonetheless, Solidworks offers more possibilities for objective functions than Creo Parametric. These objective functions can be selected in tandem with a set of design constraints:

1. Maximum displacement
2. Mass constraint
3. Frequency constraint
4. Maximum Von Mises stress

As is obvious, the topology optimisation in Solidworks is mainly focused on mechanical optimisation of a design, where it cannot consider the thermal properties of a system. This focus on the mechanical optimisation is also evident in the boundary conditions available such as fixed constraints, rollers and applied torques. Dissimilar to COMSOL, Solidworks has a section dedicated to the ensuring of manufacturability. These options include structural member size, symmetry, demolding direction and preserved areas, making Solidworks a good fit for designs which are intended to be manufactured.

Lastly, there is the aforementioned issue of having to export the resulting topology optimised geometry for a verification analysis of the design. Verifying the result in Solidworks is a suboptimal process, and therefore requires an exporting of the geometry for its verification.

3 Topology Optimisation in Solidworks

The applications and limitations of the relevant softwares have been considered. These considerations will be used in selecting a software to optimise the FPA in. Considering that Creo Parametric does not purely perform a topology optimisation on a design and its limited capabilities for objective functions, this software will not be used. If one would regard the possibility of topology optimisation for both COMSOL and Solidworks, COMSOL would allow for an optimisation in which both mechanical and thermal system characteristics are considered; whereas Solidworks would only allow for mechanical optimisation. Optimisation in COMSOL would allow for more flexibility in the objective function, and thus a consideration of both mechanical and thermal objectives as well as constraints. It is therefore that COMSOL is a preferred software to perform topology optimisation in over Solidworks, however due to limitations within the research, the optimisation module in COMSOL was not available, and therefore Solidworks was chosen as the software in which to optimise the FPA.

Solidworks has extensive documentation on their product, including the topology optimisation feature. This documentation is however not sufficient to understand the methods employed for topology optimisation, such as what optimisation solver they use, or what the exact objective functions are for which they solve. To still get a grasp of the functioning of topology optimisation in Solidworks, several test cases, employed to show the functioning of the software, are performed. These test cases aim to clarify the working of the three different objective functions in Solidworks. By understanding them, one can confidently make a decision on which objective function is most suitable for an FPA and explain the acquired result. It has to be noted again that Solidworks does not fully disclose which optimisation solver it employs or how it defines the objective functions which are represented as goals in the software. Therefore, based on the theory described in the sections 2.1.1, 2.1.2 and 2.2.1, an educated assumption is made on the approach Solidworks uses, and from that assumption, the test cases will be mathematically scrutinised. Additionally, practical considerations will be treated in this section to identify the functioning and proper application of the objective functions in Solidworks.

3.1 Optimisation Solver

An educated assumption will be made on what solver Solidworks employs in their topology optimisation study. To verify which solver Solidworks uses, output files on the density updates of each element at each iteration are desired. By being able to identify the density values an element takes on, one can reverse engineer the method with the specified jump limit and damping factor. The only output files that are available are the values of the objective function at each iteration and the final element densities. This is therefore not sufficient to verify which one is used. Another method, previously hinted to in sections 2.1.2 and 2.1.1, are the speed and behaviour of the convergence and its ability to handle multiple active constraints. Of paramount importance is that the constraints are active, as inactive constraints do not hamper the OC method.
In OC, individual, element wise sensitivities are calculated and the elements are updated separately from other elements, making the OC method dependent on the size of the element volume. MMA on the other hand, considers the system as a whole. The optimisation problem is defined such that the element wise update is determined by the element sensitivity but also by the sensitivities and constraints of all other elements. This would cause the topology optimisation to

be less dependent on the mesh size. Additionally, the OC method is unable to handle multiple constraints if they are active, as multiple Lagrange multipliers are considered separately, leading to oscillatory behaviour around the constraint. In contrast, MMA is able to handle multiple constraints, but is dependent on the chosen asymptote values and other parameters. The behaviour of convergence was therefore checked using a multiple constraints case using the Best Stiffness to Weight Ratio (BSWR) objective function, the convergence graphs can be seen in appendix A. The graphs show an oscillatory behaviour and the postulation that Solidworks uses a method which is OC, or relies on OC, can be justified. It must be stated however that the creator of Solidworks can have made adjustments to the OC method described, which could affect the solvers behaviour and lead to inexplicable behaviour.

This assumption has implications on the rhetoric used in the following section, which aims to describe the functioning of the objective functions by means of a theoretical analysis. Although the theoretical analysis is reliant on the assumption, the practical aspects of the following objective functions can be seen as independent of the assumption. The following sections treat Solidworks and its objective functions as using OC.

3.2 Best Stiffness to Weight Ratio

The first and default objective function within Solidworks is the 'Best Stiffness to Weight Ratio'. This ratio employs the equation for the total strain energy 14 as its objective function. The ratio the BSWR objective function minimises is defined as follows:

$$J(\rho) = \frac{m}{K(\rho)} \tag{21}$$

Minimising the above equation would either decrease the mass or increase the stiffness. A volume constraint is predefined and dictates how much mass can be removed. This constraint is default and cannot be turned off. The minimisation of the ratio would only consider the minimisation of the compliance, as the mass is set to a predefined value and is not optimised for.

The 'steering' of this objective function can be explained by investigating its sensitivity analysis. Additionally, a physical reasoning of what minimising the total strain energy implies can also be used. As already mentioned in section 2.2, the gradient with respect to element density is described by equation 18. Similar to equation 14 describing the total strain energy, elements with high density contribute a greater amount to the total strain energy than low density elements. Similarly, elements which experience a large strain energy, will tend to have greater densities. This concept has already been discussed in section 2.2.1. Elements in the load path of a structure often exhibit higher strain energy, leading to those elements in the load path to retain full density. The preservation of the load path leads to a structure which is inherently connected.

The idea of being inherently connected is described as that the elements in a model are all part of the same domain and there are no islands or chequerboard patterns in the optimised design. This is an important quality in assessing the usability of a design, not only in being able to export the design, but also as a telltale sign that somehow the algorithm deemed the disconnected island of geometry as contributing significantly to the design.

The reason that minimising the total strain energy will create an inherently connected structure is illustrated in a clamped-clamped beam problem with a body force (gravity) applied to it. The postulation is that a clamped-clamped beam which is connected in the middle has a lower total strain energy than a clamped-clamped beam in which there is a cut in the middle. The example is illustrated in the figure below:

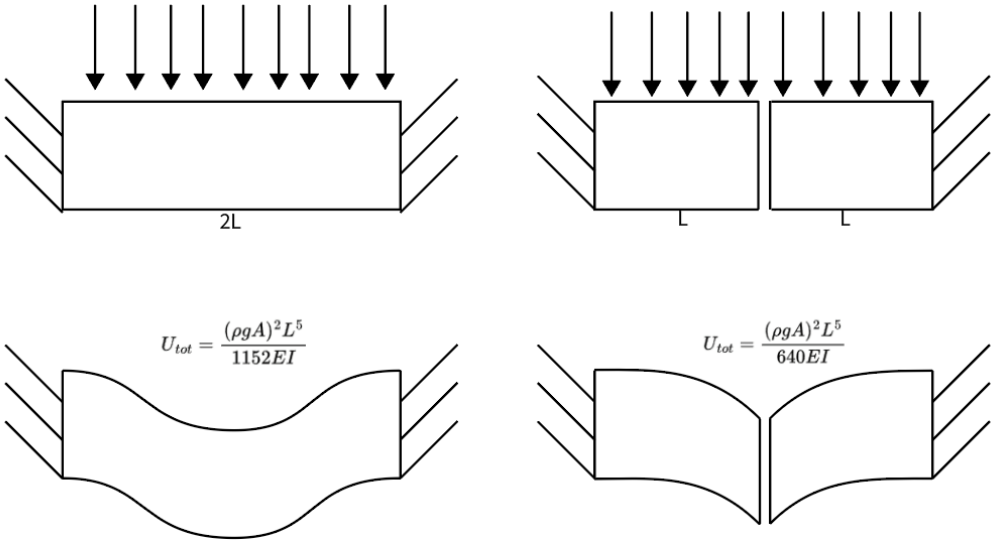

Figure 4: showing the clamped-clamped beam comparison between a connected beam and two cantilever beams.

The figure above shows the difference between deformation modes of a clamped-clamped beam and two cantilever beams and is accompanied with the equations for the total strain energy in the beams. Evident is that the connected beam has a total strain energy which is almost two times smaller than the total strain energy of the two cantilever beams added together. The above example illustrates what is expected from minimising the total strain energy of a design in topology optimisation: an inherently connected structure.

The same setup as the clamped-clamped beam as shown in figure 4 is created as a test case in Solidworks to confirm the functioning of the objective function. A diagram representing the model can be seen in the figure below.The figure below will also be used as the model in the following sections discussing the other objective functions.

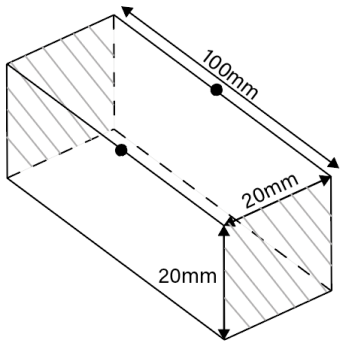

Figure 5: showing a diagram of the CAD model, its dimensions, relevant nodes, and the fixed boundaries.

The figure above shows the clamped sides as being a shaded parallelogram, the dimensions and two nodes defined at 50mm along the length of the beam. The nodes will be used in subsequent sections to measure the displacement at their positions. The beam material was chosen as copper and a body force of 60g was applied to the model. The goal chosen was the BSWR and the volume constraint was reduced to show the working principle of the objective function. The data as acquired from the simulations, which includes mass, total strain energy and stiffness to weight ratio can be found in the appendix B. The mesh size was taken as 2mm for the element dimensions. Important to note is that the results are assumed to be reproducible and constant, hence a repetition case in which the same topology optimisation with the same mesh size was performed, to verify if the solution changes, for the data see appendix C.

The benchmark of the BSWR objective function can be seen in the figures below.

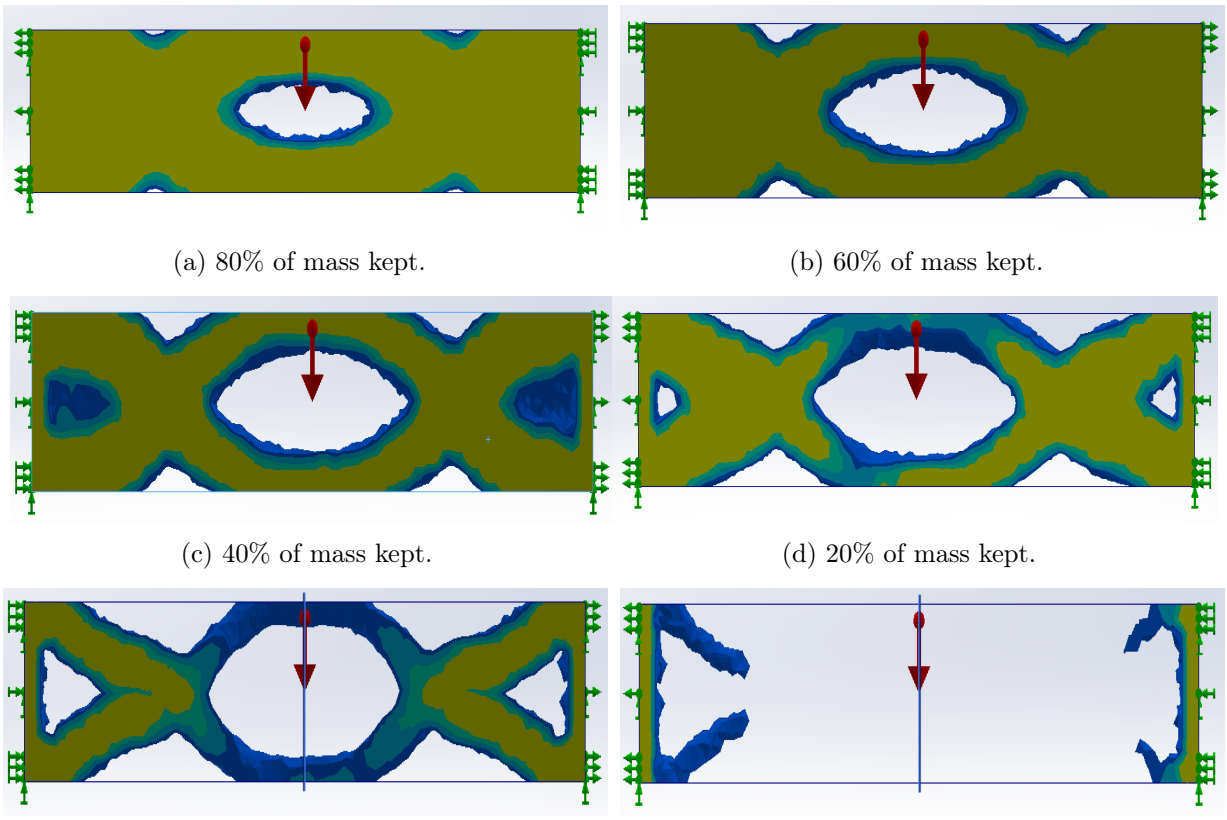

(a) 80% of mass kept.

(b) 60% of mass kept.

(c) 40% of mass kept.

(d) 20% of mass kept.

(e) 10% of mass kept.

(f) 5% of mass kept.

Figure 6: showing the evolution of the clamped-clamped beam with a body force applied to it using the BSWR objective function whilst changing the % of mass kept constraint.

Evident from the figures above is that as the volume constraint dictates a smaller amount of volume be retained, the structure, throughout figures 15a through 6e, remains connected and by approximation symmetric. It is only in figure 6f that one observes that the structure is no longer connected and the members which connected the two clamped ends in previous cases are no longer attached. This indicates that the volume constraint would be violated if the two fixed ends were attached by a member connecting them. Figure 6f is an example of how the inherent connectivity is not guaranteed if a constraint would be violated because of it. It also indicates that there is a limit to how much volume can be removed before the design becomes unfeasible. It must be noted that the objective function, whilst it minimises the 'ratio of stiffness to weight', and seems to lower this value more when more mass is removed, does not strictly improve the stiffness of the structure. The ratio is minimised, explaining why lower volume constraints yield lower ratios, so that there are two factors in play that can minimise the ratio.

There is no conclusion that can be drawn on when a design will start becoming incoherent, as this is dependent on the geometry, mesh size and added constraints; nonetheless it is worth mentioning that this is a considerable risk to take into account when selecting a volume constraint. Lastly, the coherency of the design is also dependent on mesh size, in which a coarse mesh will handle the optimisation in a coarser manner, leading to incoherent results. The ISO views of the clamped-clamped beam test cases can be found in appendix D.

The findings indicate that the BSWR objective function creates inherently connected structures as the volume constraint is reduced to lower values, up until a point where it is no longer feasible to create a connected structure. This objective function is therefore useful in creating optimised designs where connectivity is important. Additionally, the eigenfrequency of a system is directly related to the stiffness of said system, which is in turn related to the total strain energy. This relation makes the BSWR objective function also useful in preserving an eigenfrequency which does not violate the constraints on the system.

3.3 Minimise Maximum Displacement

The second objective function of interest is the minimise maximum displacement in which a nodal displacement is minimised. The node whose displacement must be minimised is either selected automatically or can be defined by the user. The measured displacement can be defined in any axis or as the geometrical norm of the three axis; a combination of two axes cannot be selected.

The objective function is hypothesised to be

$$J(\rho) = u_{nk} \tag{22}$$

In which the u_{nk} describes the nodal displacement in direction k. Important here is the difference in notation, where n represents a node of element e. The geometrical norm of the nodal displacement is of course only considered if specified in the objective function, where u_{nk}, u_{nl} and u_{nm} are presented as the displacements in the three principal directions. As seen before in section 2.2.1, the displacement tensor is related to the stiffness and force tensors as such:

$$\mathbf{u} = \mathbf{K}^{-1}\mathbf{F} \tag{23}$$

Where in this case the stiffness tensor is a function of the material density, as described in equation 13. Performing a sensitivity analysis with respect to the element density will yield:

$$\frac{d\mathbf{u}}{d\rho_e} = -\mathbf{K}^{-1}\frac{d\mathbf{K}}{d\rho_e}\mathbf{u} \tag{24}$$

$$\frac{d\mathbf{u}}{d\rho_e} = -\mathbf{K}^{-1}p\rho_e^{p-1}\mathbf{K_e^{(0)}}\mathbf{u} \tag{25}$$

$$\frac{d\mathbf{u_{nk}}}{d\rho_e} = -\mathbf{v_e}^T p\rho_e^{p-1}\mathbf{K_e^{(0)}}\mathbf{u_e} \tag{26}$$

The force tensor is independent of the element density and its derivative is therefore zero. The vector $\mathbf{v}^T$ is defined as the adjoint vector projecting $\mathbf{L} = \mathbf{K}$ onto one principal direction $\mathbf{e_k}$. The above equation resembles the sensitivity as seen in 18, where only the transpose of the displacement tensor is now the adjoint. The important part of the above equation is the fact that the derivative of the displacement tensor is a function of the global stiffness tensor. Important to note is the difference between equations 18 and 26 is the fact that the former considers a global value, whereas the latter only a local one. The sensitivity of the above objective function is much akin to the sensitivity of the BSWR. It is therefore expected that the minimise displacement objective function also creates a connected structure. The structure is however not optimised for a

global stiffness, but the global stiffness is rather optimised for a stiffness resulting in a minimum displacement at a given node.

Secondly, a more practical consideration, is that the selection of the nodes for which to minimise the displacement is of key importance in the topology optimised result. An asymmetry in the selection of the nodes can lead to compliant mechanisms, where some parts displace greatly such that others parts may remain stationary. Another aspect to this, is that not selecting a node for which to minimise displacement, will lead to the removal of material at that node. This is of course use case specific, but the consequence of it will be shown in the test cases below. The test case uses the same model as shown in figure 5. The nodes visible in the middle of the beam in figure 5 are selected as the nodes for which to minimise the displacement. In the test case, a mesh size of 2mm was used again. The nodal displacement data can be found in appendix E

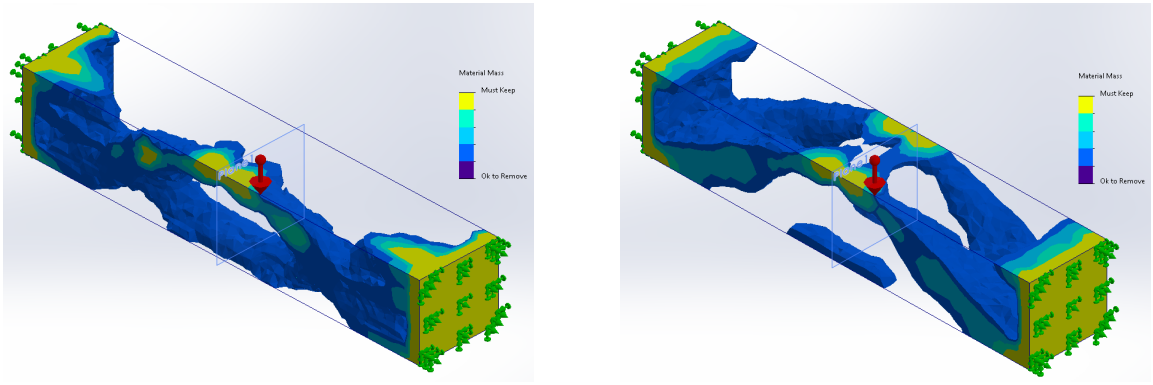

(a) One node selected, 20% of mass kept.

(b) Two nodes selected, 20% of mass kept.

Figure 7: showing the difference between the results as the displacement of one node as compared to two nodes is minimised, when 20% of the mass is kept.

As seen in the figures above, the difference is obvious. Figure 7a shows that material is only kept at the node which has been selected to optimise for. Figure 7b shows that both nodes are considered and that the result shows some symmetry. The prioritization of the displacement at the selected nodes can also be seen when looking at the displacement field of the whole model. For this purpose, the average displacement and the displacement field for the one-node and two-node case are shown below.

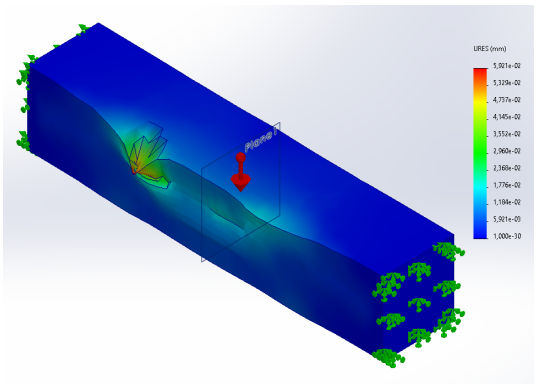

(a) One node selected, other side of model is shown, 20% of mass kept.

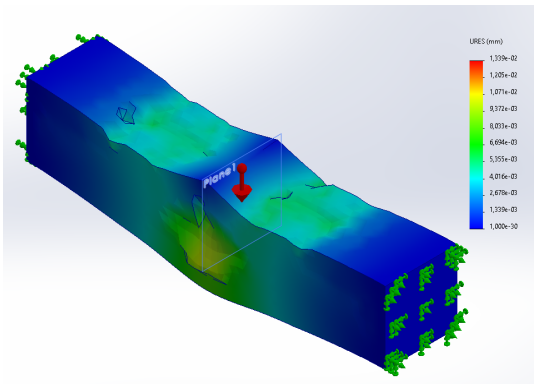

(b) Two nodes selected, 20% of mass kept.

Figure 8: showing the difference between model displacements as the displacement of one node as compared to two nodes is minimised, when 20% of the mass is kept.

Essential to understanding how the displacement is presented in Solidworks is the following quote as stated in the Solidworks User Interface:

> "The values are based on the entire model which may contain porous elements that are less rigid than fully dense elements. For this reason the values should be thought of as a rough estimate on how the final model might behave"

The figures as shown in 8 show the displacement of the model as if all elements were still present, but just with differing densities. As previously mentioned in section 2.2.1, to avoid numerical issues, elements are not removed but kept at a minimum density. In the models shown in 7, elements with densities greater than 0.3 are shown and are accounted for, whereas in figures 8, all elements are shown, and just their stiffness tensor is defined differently. It is therefore that in 8a, a displacement is shown where the material densities are less than what the Solidworks interface shows by default.

Benchmarking the minimise displacement objective function has shown that an inherently connected structure is created, but that the global stiffness is only meant to minimise the displacement of a single node. Additionally, the objective function is also sensitive to asymmetry in the design, as showcased in figures 7a and 7b. The objective function is only useful when a nodal displacement must be minimised, but where other displacements in the model are allowed.

3.4 Minimise Mass

Minimising mass is a straightforward method of removing as much mass as possible. Understanding what designs the objective function yields is key to drawing conclusions on its usefulness and how well it can be applied to an FPA. The proposed objective function is:

$$J(\rho) = \sum_{e=0}^{N} \rho_e v_e \tag{27}$$

Which is simply the mass of the design that is to be minimised. Its gradient is therefore:

$$\frac{J(\rho)}{\rho_e} = v_e \tag{28}$$

The sensitivity of the objective function is therefore plainly the element volume, which is a constant. An unconstrained optimisation with this objective function would therefore lead to all material being removed. This objective function is therefore only applicable with suitable constraints; a volume constraint is not possible. The only constraints which are then possible are the frequency, displacement and stress constraints. In this discussion, the active or inactive nature of a constraint is of key importance.

3.4.1 Frequency Constraint

Firstly, the mass minimisation objective function is combined with the frequency constraint. This constraint dictates the first eigenfrequency of the model, where it can assume a greater than, lesser than or in between constraint. Firstly, the greater than constraint is considered and applied to the model as seen in figure 5. A static study showed that the reference eigenfrequency of the model is 5908.5Hz. It is known from theory that a beam longer in length will have a lower eigenfrequency than one which is shorter. The cross-sectional area of a beam will also influence the eigenfrequency. As the cantilever beam gets shorter, the frequency increases, which is desired for a greater than frequency constraint and hence, this constraint is inactive and will result in an inherently disconnected geometry. The constraint was tested for a frequency greater than 2000Hz, 4000Hz and 6000Hz; all simulations resulted in the same geometry and therefore only one will be shown.

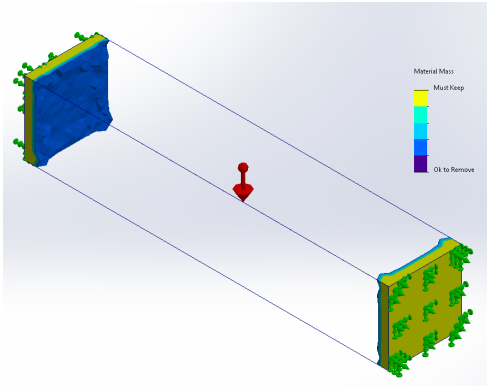

Figure 9: showing the resulting geometry for a frequency constraint greater than 4000Hz using the mass minimisation objective function.

Evident from the figure above is that the geometry is disconnected. The resulting geometry was found to have an eigenfrequency of 28578Hz, far higher than the required constraint. The simulations with the other constraints also yielded the same eigenfrequency of the optimised model. This model incoherency can be explained when regarding the nature of the eigenfrequency calculation in Solidworks. In section 2.2 it was indicated that elements cannot be void but retain a minimum density. If all elements appear as 'removed', they are actually at the minimum allowable density and still contribute to the global stiffness of the structure. Because the rigid parts

of the beam as seen in figure 9 are short and their cross sectional large, the eigenfrequency of the beam is dominated by these elements. The minimum density element are still considered in the eigenfrequency calculation, but contribute a negligible amount to the stiffness, causing the eigenfrequency to become unreasonably high. This notion is important when considering the less than eigenfrequency constraint.

Unlike the greater than eigenfrequency constraint, the lesser than constraint imposes a constraint which is more likely to be active. Because shortening the beam leads to a higher frequency, this 'method' cannot be employed as this would violate the frequency constraint, which would lead to a design that is dissimilar to that seen in figure 9. Nonetheless, the important notion that elements are not void and still contribute to the global stiffness can also be employed here. Beams with a mass at the end are shown to have a lower eigenfrequency than uniform beams. Beams with element densities higher at the end of the beam and lower densities in between the fixed end and the end will therefore also have a lower eigenfrequency. By this rhetoric, islands elements with densities higher than the minimum density are created as far away from the fixed ends as possible to artificially lower the eigenfrequency of the system.The minimise mass objective function in combination with several less than eigenfrequency constraints was benchmarked and the results can be seen in the figures below.

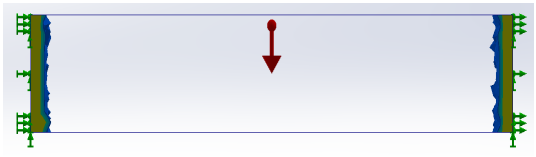

(a) <6000Hz, relative densities ≥ 0.3.

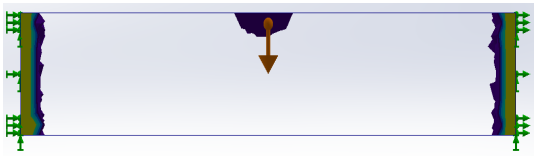

(b) Actual <6000Hz, element densities $> \rho_{min}$.

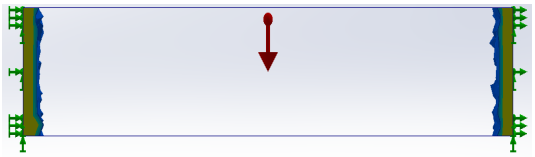

(c) <4000Hz, relative densities ≥ 0.3.

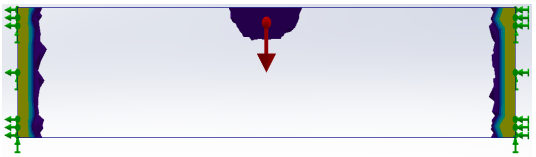

(d) Actual <4000Hz, element densities $> \rho_{min}$.

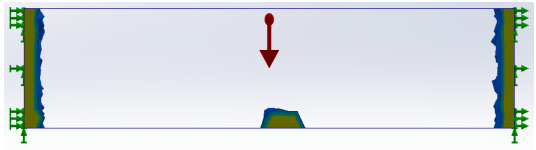

(e) <2000Hz, element densities ≥ 0.3.

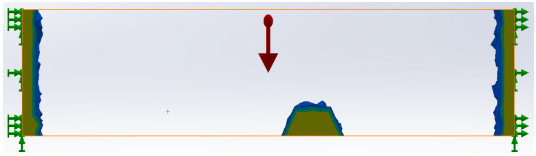

(f) <1000Hz, element densities ≥ 0.3.

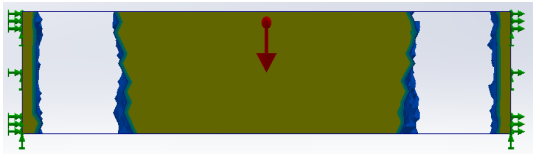

(g) <100Hz, element densities ≥ 0.3.

Figure 10: showing the resulting geometries for less than frequency constraints.

As seen in the figures above, as the constraint on the frequency becomes tighter, Solidworks finds

a way to work around it by defining the geometry as such that it can achieve the constraint. It is especially in figures 10a, 10b and 10c, 10d that this 'cheating' of the frequency constraint is observed. Figure 10a shows all elements with a relative density larger than 0.3, whereas figure 10b also shows some elements with a smaller density. The elements with density equal to ρ_{min} are not shown. The elements with the lowest allowed density also contribute to the total stiffness of the system, albeit a negligible amount, but do connect the island as seen in the middle of figure 10b. Due to this small, but not negligible element stiffness, the island that is created contributes to the first eigenfrequency of the system, effectively lowering it as compared to what the first eigenfrequency would be when only the two fixed slabs remain, as seen in figure 9. As the constraint becomes stricter and lower frequencies are desired, Solidworks 'cheats' more by creating islands whose elements have a density of higher than 0.3 and are therefore visible in figures 10e, 10f and 10g. This phenomenon can be explained using the same idea discussed previously that a beam with a mass at the end has a lower first eigenfrequency than a uniform beam. The figure in 10g can be regarded as a large mass attached to a flexible beam, causing the eigenfrequency to be low. The results above also display a higher mass. The measured frequency and mass of the test cases are shown in the table below.

Table 1: Table showing the frequency constraints, the resulting first eigenfrequency and the mass.

Less than [Hz]	6000	4000	2000	1000	100
Frequency [Hz]	5927.8	3973.6	1986.8	999.82	171.26
Mass [kg]	0.01138	0.01138	0.01151	0.1201	0.20670

As indicated in the above figure, almost all frequency constraints are satisfied except for the $< 100Hz$ frequency. The contribution of the created islands to the eigenfrequency is illustrated in the mode shape plots of the model, which considers the displacement of the entire model in its first eigenfrequency. These figures are shown below.

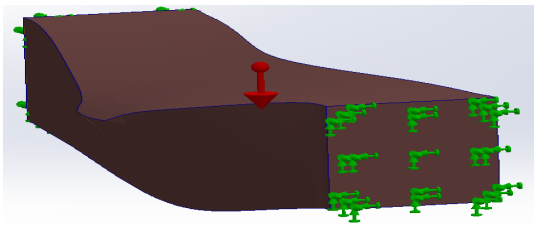

(a) <6000Hz mode shape.

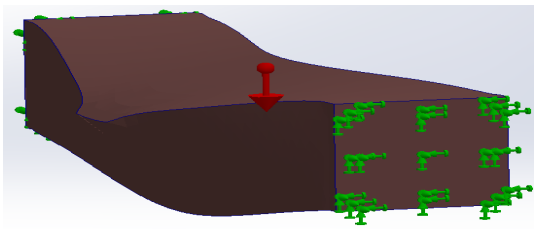

(b) <4000Hz mode shape.

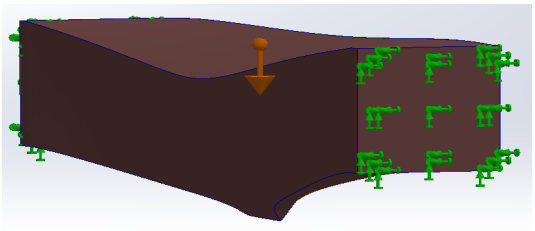

(c) <2000Hz mode shape.

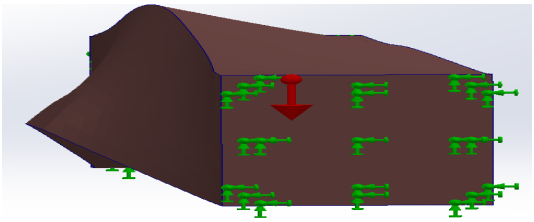

(d) <1000Hz mode shape.

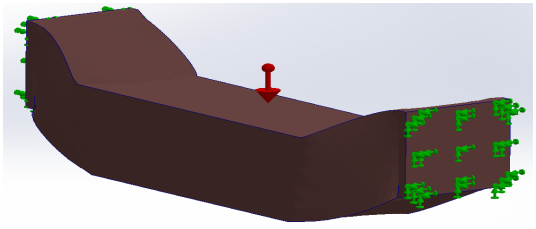

(e) <100Hz mode shape.

Figure 11: showing the mode plots for the frequency constrained optimised models using the mass minimisation objective function.

The above figures illustrate how the islands that are seen in figure 10 act as rigid bodies in the mode shape plots, enforcing the impression that it is because of these islands that the frequency constrained is able to be achieved. The elements with element density equal to ρ_{min} deform in a more continuous manner, akin to the mode shapes as seen in the appendix F. It is especially obvious in figure 11e that the middle, rigid and full density part of the optimised model does not deform but rather it is the elements connecting the fixed ends and the middle that deform. This creates a mass suspended by a flexible material, leading to the low eigenfrequency. For reference, the mode shape plots of the reference beam and the result as shown in figure 9 can be found in appendix F.

Another thing to note is the position of the island creation. In figure 10f for example, the island is created in the bottom of the beam, however, reruns of the simulation showed that the island can also be at the top of the beam, or on the 'left' or 'right'. Theory supports that the island will be created in the middle between the two fixed ends, as it will decrease the eigenfrequency the most.

3.4.2 Displacement Constraint

The second constraint with which to test the mass minimisation objective function is the displacement constraint, which limits the nodal displacement of selected nodes to a certain value. In this section and in section 3.3, the sensitivity of both the mass and the nodal displacement have been analysed. The Lagrangian of this optimisation problem is described by:

$$\frac{dL(\rho,\lambda)}{d\rho_e} = -v_e + \lambda_e \frac{df(\mathbf{K_e},\mathbf{u})}{d\rho_e} \tag{29}$$

In which the $f(\mathbf{K_e},\mathbf{u})$ is the sensitivity function of the nodal displacement. If the objective function, v_e in this case, is larger than the sensitivity of the constraint times the Lagrange multiplier, it will be favourable to remove those densities, as it will reduce the mass of the system, whereas if the second term is larger, the element density will tend to increase. This makes this combination of objective function and constraint mesh dependent. To test the hypothesis that the 'steering' of the solver, or the ability to make an inherently connected design, is dependent on the mesh size, several mesh sizes were tested for the same constraint. The figures below show the progression of the results as mesh size is decreased. The displacement of the nodes and the corresponding masses can be found in appendix G.

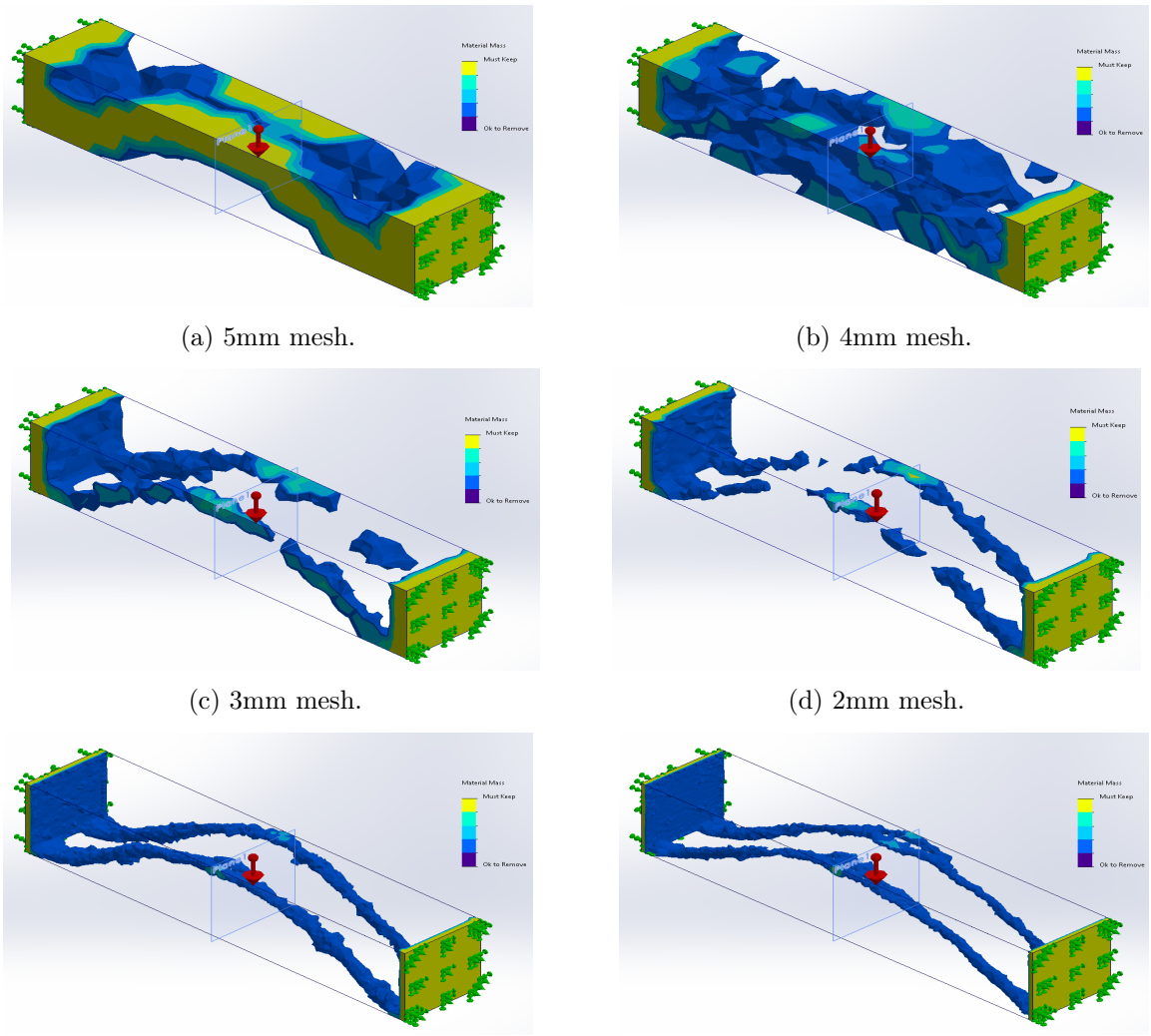

(a) 5mm mesh.

(b) 4mm mesh.

(c) 3mm mesh.

(d) 2mm mesh.

(e) 1mm mesh.

(f) 0.75mm. mesh

Figure 12: showing the resulting geometry of the mass minimisation objective function in combination with a displacement constraint as the mesh size is decreased.

The figures above show a convergence to a structure resembling two arcs that lead up to the nodes for which to minimise the displacement. The coherency of the structure seems to worsen from 5mm to 2mm, but improve for the cases of 1mm and 0.75mm. This improvement of coherency goes hand in hand with an exponential increase in computational time, as a mesh size of 0.5mm exceeded the 24 hour runtime. In the case where the mesh size is 5mm in figure 12a, the structure shares some semblance to the models shown in smaller mesh sizes, when the mesh size is further decreased to 4, 3 and 2mm, the creation of islands and incoherency increases. Only in mesh sizes of 1mm and 0.75mm does the model regain some coherency. It is therefore postulated that the mass minimisation objective function in combination with the displacement constraint can only produce coherent results if the mesh size is small. How small is left untreated in this research, but important to note is that the computational time increased significantly. A mesh size of 0.5mm led to a run time of longer than a day, after which Solidworks quit the computation. To confirm the dependence on the mesh size of the mass minimisation objective function, decreasing

the mesh size was also tested in combination with the BSWR objective function. The results indicated that the BSWR objective function retained coherency in larger mesh sizes. The results of this meshing test can be seen in appendix H.

3.4.3 Von Mises Stress Constraint

The von Mises stress constraint specifies the maximum amount of von Mises bstress that can be present at any point in the model. It is defined as a percentage of the yield strength of the material. The mesh is required to be small and of high quality as to avoid the build up of stress in mesh elements that are too large. Decreasing mesh size increases computational time and cost significantly, which is often, for complex designs, a limiting factor. The von Mises stress is defined as a sum of differences in the principal stresses, which are related to the strains of the elements in the model. It is hypothesised that, similar to the frequency constraint, the mass minimisation objective function 'cheats' the constraint by removing all material in between the fixed areas because the stress constraint is inactive for lower stresses. The stress is highest near the corners of the fixed areas, as the displacement is most constrained there. If the value of the von Mises stress at that node is lower than the yield strength of the material, the optimisation will yield an empty result and only the fixed ends will remain.

A static study showed that the highest von Mises stress, with a 60g load, was measured at $2.165 \cdot 10^6$MPa, which is two orders of magnitude lower than the yield strength of the material. The resulting geometry only showed the two fixed areas with nothing in between, similar to figure 9. Confirming that because the constraint is inactive, the mass minimisation objective function will reduce the mass to the minimum amount possible. This result is dependent on the initial conditions of the system, e.g. the source of the stress. As the load is increased to unreasonably large amounts, the original model will show a von Mises stress which is in the same order of magnitude as the yield strength. If the topology optimisation is subsequently considered with this load case, an 80000g load, the constraint is assumed to become active and the objective function will not yield the design as seen in figure 9. The primary concern in this model is reducing the stress concentration that is found in the elements in the corners of the fixed areas, which it will do by 'spreading out' the stress over multiple elements to reduce the peak stress, an idea similar to what is seen in the BSWR objective function. The result of the 80000g load combined with the topology optimisation is shown below.

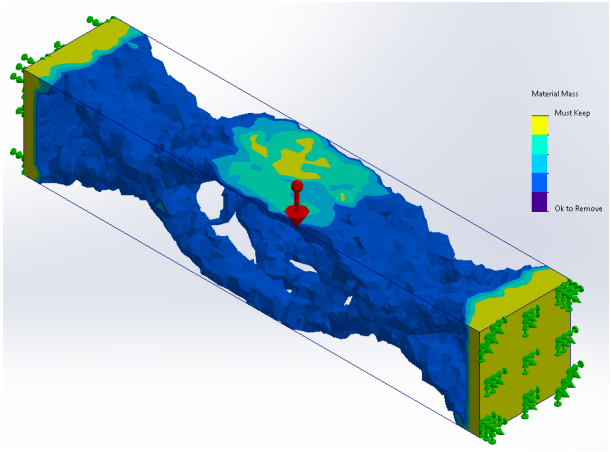

Figure 13: showing the ISO view of the resulting geometry using the mass minimisation objective function in conjunction with a maximum allowable von Mises stress of 80% and with an 80000g load applied.

It must however be noted that in the figure above, that although the constraint was satisfied, the values of the mass and stress had not reached convergence and the optimisation stopped at the maximum iteration number. The maximum von Mises stress in the model is $1.76 \cdot 10^8$ MPa. The model, as in section 3.4.2, displayed some random elements that at first sight do not logically seem to contribute meaningfully to the model, suggesting that mesh size here is also important.

Using the von Mises stress constraint in conjunction with the mass minimisation objective function is dependent on the (in)active nature of the constraint. An inactive constraint will lead to a reduction in mass irrespective of coherency. An active constraint on the other hand will impose restrictions on what material can be removed and lead to a coherent design, for the same reasoning as given in section 3.2 where strain and stress are directly related. An active constraint is again dependent on the mesh size used. This constraint has been shown to create an inherently connected result, but costs considerable resources, especially in complex designs, and will therefore not be used due to lack of resources.

This section has benchmarked the functioning of the three objective functions in Solidworks to elaborate on their strengths and limitations. The findings indicate that the BSWR objective function both theoretically and practically shows that the designs created with it are inherently connected. Optimising for the global stiffness is also directly beneficial to the eigenfrequency of the system if a high eigenfrequency is required. Reducing the total strain energy is related to increasing the eigenfrequency through the system's stiffness. The minimise displacement objective function was shown to function in a similar manner to the BSWR objective function: exhibiting an inherent connectivity and a focus on stiffness. A scrutiny of the sensitivity analysis of the objective function showed that the global stiffness affected the proposed objective function to minimise nodal displacement. Key in the sensitivity analysis was that the global stiffness was only considered to minimise the nodal displacement, and not a global function such as total strain energy. This focus on a local parameter was showcased along with the sensitivity of the objective function to asymmetries. The minimise mass objective function has been benchmarked with the three available constraints: frequency, displacement and von Mises stress. The sensitiv-

ity analysis showed a dependence on the mesh size, which was confirmed in the benchmark of the displacement constraint. Applying the frequency constraint showed that elements with ρ_{min} still contribute to the global stiffness and influenced the eigenfrequency of the system. This influence led to Solidworks 'bypassing' the frequency constraints. The von Mises stress constraint resulted in a similar rhetoric, where if the von Mises stress constraint was not active, all material was removed. Only with a high enough static von Mises stress did the constraint become active and produce an inherently connected result. Using the mass minimisation objective function in combination with the von Mises stress constraint makes the optimisation problem doubly dependent on the mesh size of the design. The mass minimisation objective function is therefore dependent on the constraints applied to the design and has been shown to inconsistently produce inherently connected structures if both the mesh size is small enough and the constraint active.

4 Optimising an FPA

Optimising an FPA requires relevant constraints on the system and what system characteristic to optimise for. The objective functions described in the previous sections optimise for stiffness, a nodal displacement and a minimal mass. However, an FPA requires more consideration, as it is not only mechanical aspects that are relevant, thermal aspects are of equal importance. There are several facets to optimising an FPA that must be identified, the first considers what physical considerations are relevant to be able to identify what to optimise for. The relevant system characteristics are identified through these physical considerations and a set of Figures of Merit will be ascertained that describe the performance of the system. The second facet concerns what optimisation method will be employed, and lastly, a model must be created to optimise. This section aims to treat all three aspects necessary to optimise an FPA.

4.1 Physical Considerations

The optimisation process requires a parameter to optimise for and relevant system constraints, these must therefore be identified for an FPA. These system characteristics must be identified from the physical principles governing the thermal-mechanical behaviour of an FPA. The relevant thermal and mechanical physics are therefore described in this section with the goal of understanding the key system characteristics for the optimisation.

4.1.1 Thermostatics-dynamics

The detector array in an FPA is a magnetically and thermally sensitive device which operates at a nominal temperature of 50mK [11]. To maintain performance of the detector array, its temperature must therefore be as close to the nominal operating temperature as possible. A heat load is consistently applied to the detector array through multiple sources, which will be discussed later, so that the detector array and the structure beneath it must be able to carry this heat away. The flow of heat $\dot{q}$ through an object of area A, with a thermal conductivity κ and a temperature gradient ∇T is given by Fourier's law of heat conduction [24]:

$$\dot{q} = -\kappa A \nabla T \tag{30}$$

Considering a simple beam with a fixed temperature on one end and a heat input on the other end, a simple temperature profile can be determined using equation 30. If one uses instead of the gradient, only the x-direction, one can solve the ODE using given BC's to obtain a linear relation between the temperature and position along the x-direction as such:

$$T(x) = \frac{\dot{q}}{-\kappa A}(x + a) + T_a \tag{31}$$

Where a is the position where one boundary condition is defined and T_a is the temperature defined at that position. The difference between the temperature at the origin and the temperature at point a is then given by:

$$\Delta T = \frac{\dot{q}}{-\kappa A} a \tag{32}$$

From the above equation is obvious that, to reduce the temperature gradient from origin to point a, the conductivity and area must be maximised, whilst the power input is to be minimised. Important to note is that the area in question is the cross-sectional area of the object through which heat is flowing.

The above section and equations only deal with static problems in which equilibrium has been reached. For an analysis about the temporal/thermal stability of an object subject to power a input, the heat diffusion equation is used. The equation describes a systems energy conservation and is shown below [24]:

$$\dot{E}_{in} + \dot{E}_g = \dot{E}_{st} + \dot{E}_{out} \tag{33}$$

Where $\dot{E}_{in}$ describes the rate of energy into the control volume, $\dot{E}_g$ the rate of energy generated within, $\dot{E}_{st}$ the rate of energy stored within and $\dot{E}_{out}$ the rate of energy leaving the control volume. Ignoring internal energy generation[24], one can write the above equation, using equation 30, as:

$$\kappa \nabla^2 T = \rho C_{eff} \frac{\partial T}{\partial t} \tag{34}$$

Where the LHS is responsible for the flow of heat throughout the control volume, being derived from $\dot{E}_{in} - \dot{E}_{out}$, and the RHS is the rate at which energy is stored inside the control volume with ρ as the material density and C_{eff} as the volumetric or effective thermal capacity. Equation 34 can also be applied to a one dimensional case, giving:

$$\kappa \frac{\partial^2 T}{\partial x^2} = \rho C_{eff} \frac{\partial T}{\partial t} \tag{35}$$

This partial differential equation (PDE) can be solved using given boundary conditions for temperature, heat flux, insulation or convection. Solving equation 34 is time consuming. The system is therefore described in a manner making it easier to predict its behaviour. The system will be described as an RC circuit. This analogy will help simplify the thermal behaviour and allow for the determination of further important thermal system characteristics.

4.1.2 Thermo-electrical Analogy

To simplify the otherwise complex nature of the thermal system, an analogy is made between a thermal system and an electrical circuit [25]. These systems, although not apparently akin, can be described using similar physics, which is what the thermo-electrical analogy is built upon.

The similarity in physical behaviour can be found in the resemblance of equation 34 to the equation describing the 'rate of voltage rise' [25], as described by Robertson and Gross:

$$\frac{\partial v}{\partial t} = \frac{1}{rc} \frac{\partial^2 v}{\partial x^2} \tag{36}$$

Where the LHS is the 'rate of voltage rise' and the RHS contains r is the circuit resistance, c the circuit capacitance and $\frac{\delta^2 v}{\delta x^2}$ describes the Laplacian operator in one dimension.

The resemblance between equation 35 and equation 36 is obvious, where the thermal conductivity is analogous to the inverse of the electrical resistance, and the effective thermal capacity is analogous to the electrical capacitance.

The analogy allows one to describe a thermal system as an electrical circuit, effectively allowing one to describe the system using a transfer function as one would for a circuit. To describe the thermal system as an electrical circuit, the analogous elements must be identified: the conductivity is the resistance and the effective thermal capacity is the capacitance. Considering that the T0 housing of the FPA is made from a uniform material, it can be approximated as being a block of material with conductivity κ_h and with effective thermal capacity C_{eff} with the thermal strap attached to it also having a conductivity κ_s but negligible thermal capacity due to its comparably low mass. The inverse of the thermal conductivities is used to denote the thermal resistance. The strap is connected to a power source, the cryocooler, and is analogous to a current source. Therefore the thermal system can be described as a current source connected to two resistances in series followed by a capacitor, connected to ground. The following figure shows the thermal-electrical model for the simplified T0 housing of the FPA:

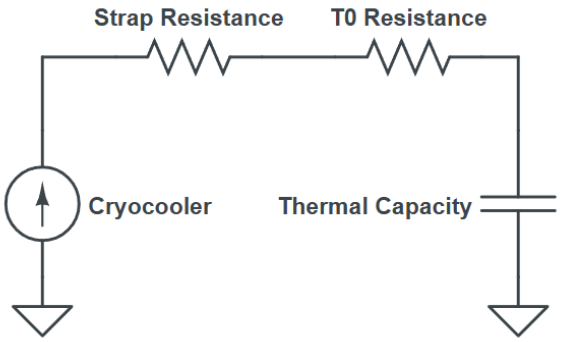

Figure 14: showing the thermal-electrical model for the simplified T0 housing of the FPA.

The above circuit is an RC circuit, with two resistances and a capacitor, all in series. The transfer function for this circuit is:

$$T(s) = \frac{1}{(R_s + R_h)C_{eff}s + 1} \tag{37}$$

Where R_s refers to the strap resistance and R_h to the housing resistance. The above system is of first order, hence the response will be too. The time constant of this circuit, which describes a fifth of the time required to reach equilibrium, is given by:

$$\tau = \frac{C_{eff}}{R_s + R_h} \tag{38}$$

The magnitude and phase response of the system are relevant because the cryocoolers duty cycle performs at a certain frequency, which if matched allows for the best cooling speed and the least energy consumed. If the thermal eigenfrequency of the thermal capacity is too low, the crycooler is unable to effectively cool down the FPA and it will require large amounts of energy. On the other hand, if the thermal eigenfrequency is too large, the control system in the cryocooler cannot adequately respond to fluctuations in the temperature of the FPA as the cryocooler is limited in

its own handling frequency. The time constant of the system must therefore be roughly equal to 1 for the optimal performance of the crycooler and FPA combination. For equation 38 to be 1, the thermal capacity must equal the added resistance of the strap and housing. In this proposed model, the strap dominates the thermal resistance of the circuit so that the T0 resistance is assumed to be negligible. The strap resistance is in the order of magnitude of $10^{-4}\frac{K}{W}$ and the optimal value for the thermal capacity would therefore be the same. In more detailed models, the contact resistance also plays a significant role, but is purposefully not considered to reduce complexity.

4.1.3 Thermal and Mechanical Properties at Low Temperatures

Material properties, whether mechanical or thermal, change as the temperature changes. For engineering purposes at room temperature without extreme temperature changes, the changes in material properties is negligible. The FPA however, operates nominally at a temperature of 50mK and the effect of temperature must be considered. Important properties for an FPA, such as the effective thermal conductivity of the material of which it is made and the effective thermal capacity are both functions of temperature [26]. The dependence of the thermal conductivities on the temperature as approximated to be a power law, for which the coefficients a and b, as seen in equation 39 have been experimentally acquired [27].

$$\kappa(T) = aT^b \tag{39}$$

For copper, the thermal conductivity scales linearly with the temperature in the relevant temperature range, but is also dependent on the treatment and purity of the Copper [14], this number is reflected in the Residual Resistance Ratio (RRR) and is in the order of 10's, a higher number representing a better purity. Many factors influence the RRR, however for the sake of brevity, it is assumed to be 30 [14].

$$\kappa_{Cu} = \frac{RRR}{0.634}T \tag{40}$$

The thermal capacity of a material is also a function of temperature. Instead of a simple power law, one can describe the specific heat as a function of temperature as a polynomial with odd values of n. The general equation for the specific thermal capacity of copper can be seen in equation 41[14].

$$C_{Cu} = \frac{1}{63.546}\sum_n A_n T^n \tag{41}$$

The values for the coefficients A_n are found in appendix I. At the operating temperatures of the FPA, the above equation can be assumed to be approximately linear, where only the first and third order term are considered as the significance of the other terms are assumed to be negligible. This leads to the specific thermal capacity of copper as a function of temperature to be described by:

$$C_{Cu} = \frac{1}{63.546}\left(0.69434T + 0047548T^3\right) \tag{42}$$

The effects of temperature on the thermal properties are of importance because the detectors used in an FPA are sensitive to fluctuations in temperature, which is directly linked to the ability of the housing to store and conduct heat, so that this ability must be described as realistically as possible to predict the behaviour of the system accurately.

The mechanical properties, although dependent on temperature [28], are assumed to be independent due to the scale at which they change. The largest change in mechanical properties is found when going from room temperature to near zero Kelvin. The mechanical properties of an FPA are only relevant during the launch, at which the FPA is not actively cooled considerably. Therefore, the mechanical properties are said to be constant.

4.1.4 Mechanics

The satellite carrying the FPA experiences no mechanical loads in orbit. The thermal considerations are only important when the FPA is operating. The mechanical considerations are important when the satellite carrying the FPA is launched into orbit. The conditions in the launcher impose several mechanical constraints on the FPA's design. This section aims to elaborate on these principles and why they are relevant.

The first relevant system characteristic is the resonant frequency of the FPA. This constraint is dictated by the launcher in which the FPA will be sent to space with. For the Ariane 6[29], the lateral frequency must be greater than 6Hz and the longitudinal frequency must be greater than 20Hz to avoid dynamic coupling. The Vega C launcher has similar requirements[30]. The concept of dynamic coupling is important in spacecraft design and is related to the amplitude amplification of eigenmodes. As a body experiences excitation in any eigenfrequency, the amplitude of the movement will be increased, leading to large deformations and stresses. Next to this low frequency constraint meant to avoid dynamic coupling, there are also higher frequencies that must be avoided, these are primarily caused by acoustic vibrations from the launch [29][30]. For the Vega C, these range from 31.5-2000Hz with 500Hz being the loudest, to avoid resonance, avoiding these frequencies is of utmost importance. There are other frequencies which are imposed on the spacecraft and launcher which are higher, but less relevant. Understanding how to design for a specific eigenfrequency is therefore crucial.

The fundament of a systems eigenfrequency lies in the equations of motion defining the system, which is dependent on time, the mass, damping, stiffness, displacement and its derivatives and an external force. This one dimensional system can be regarded as a mass-spring-damper system.

$$M\ddot{x}(t) + C\dot{x}(t) + Kx(t) = f(t) \tag{43}$$

If external forces and damping are neglected, the system is reduced significantly. Assuming the displacement is harmonic, the frequency is found by solving the eigenvalue problem of the equation and eventually yields the frequency dependent on the systems stiffness and mass[31].

$$f = \frac{1}{2\pi}\sqrt{\frac{K}{M}} \tag{44}$$

The above equation defines the frequency of a mass-spring system with a certain harmonic displacement in one DoF. Generalising this system to multiple degrees of freedom leads to [31]

$$0 = |\mathbf{K} - 2\pi f_j \mathbf{M}| \tag{45}$$

This indicates that the eigenfrequencies are still dependent on the individual stiffnesses of the masses and the masses themselves. A lower mass will lead to an increase in the frequencies of the system and vice versa. Most cases are not that straightforward, where lowering the mass can also lead to decrease in the frequency. For a simple cantilever beam, the eigenfrequency can be described using

$$f_i = \frac{n}{2\pi}\sqrt{\frac{EI}{\rho A L^4}} \tag{46}$$

The above equation indicates an importance of the distribution of mass, indicated by the moment of inertia I, and the materials Young's modulus in determining the eigenfrequencies. The variable n represents a constant which is inherent to the mode shape. A and L represent the area and length of the beam.

During the launch, the launcher accelerates to reach the escape velocity. The acceleration in combination with other, random, loads causes a thrust and subsequently a force on the payload which is assumed to be quasi-static. The load is still time dependent but applied slowly enough to be approximated as static. This load is called the Quasi-Static Load (QSL) and is in this context used to describe the maximum g force experiences by the FPA [32]. This load is applied longitudinally and laterally and is measured in the amount of g's applied. The applied load to the FPA causes a deformation and consequently stresses the material. Because the FPA housing is said to be made of a metal, a good measure of the stress built up in the housing is the von Mises stress:

$$\sigma_{vm} = \sqrt{\frac{(\sigma_1 - \sigma_2)^2 + (\sigma_2 - \sigma_3)^2 + (\sigma_3 - \sigma_1)^2}{2}} \tag{47}$$

The above equation only considers the principal stresses in a system. It is imperative that the von Mises stress does not exceed the value at which the material will fail: the yield strength. Therefore, a constraint is also imposed on the maximum von Mises stress an FPA can display. A large number of safety and design factors are imposed on the maximum allowable von Mises stress so as to ensure the safety of the design.

This section aimed to detail the relevant physical theories for an FPA, which were shown to be both thermal and mechanical. The relevant thermal considerations concerned the effective thermal conductivity of the T0 housing to be able to conduct heat away from the detector array towards the thermal strap. Additionally, the thermal model has been simplified to an RC circuit, which aimed to simplify the model of the temporal response of the T0 housing. This thermo-electrical analogy showed that the thermal strap resistance dominates the resistance of the circuit, and to get a preferable temporal response of the T0 housing, its capacitance must be comparable. Mechanically, the FPA is influenced by the launcher conditions, imposing constraints on both the eigenfrequency and maximum von Mises stress of the system. The eigenfrequency is influenced by the stiffness of the system and its moment of inertia, both of which are influenced by the geometry of the design. The von Mises stress is also directly related to the geometry of the design, where sharp corners can increase local stress. The system only contains mechanical constraints

and no characteristics to optimise, whereas thermally, the system contains characteristics for which it can optimise.

4.2 Boundary Conditions, Constraints and Figures of Merit

Having discussed the relevant thermal and mechanical physics, the important system characteristics can now be identified. The distinction between a system characteristic to optimise for and one to consider as a constraint is important. The constraints originate from the launcher conditions and the operating mode of the FPA in space. The boundary conditions and constraints are listed below.

- The FPA shall have a resonant frequency higher than 200Hz
- The FPA shall withstand a lateral QSL of 60g
- The FPA shall withstand a longitudinal QSL of 60g
- The FPA shall have a von Mises stress lower than 80% of the yield stress of copper
- The detector array will carry a heat load of 20nW
- The aramid connections shall each carry a heat load of 300nW
- The thermal strap shall have a temperature of 50mK

The above lists the system characteristics which are constrained. The mechanical system characteristics are listed as constraints rather than ascertaining them as parameters to optimise. The eigenfrequency and maximum allowable von Mises stress should adhere to a certain threshold value, but there is no considerable advantage for the performance to having them exceed or remain below it. The mechanical system characteristics are therefore posed as system constraints for an FPA. Only the mass and thermal system characteristics remain to describe the performance of an FPA. Therefore, the Figures of Merit concerned with assessing the performance of an FPA will only consider the thermal system characteristics.

The temperature of the detector array and its temporal stability are described by the effective thermal conductivity of the FPA and its effective thermal capacity. These are good system characteristics to be classified as FoM as they describe how well heat flows through the FPA and is stored within it. Important to note is that these FoM are defined through effective system properties, the thermal conductivity and thermal capacity of a material do not change if geometry is changed, but the effective thermal conductivity and effective thermal capacity do, as they are relative measures of how well heat is conducted or stored in a given direction based on geometry. The effective thermal conductivity is a system characteristic which is dependent on the geometry and should be optimised for to improve the performance of the detector array. The effective thermal capacity is a system characteristic whose value should be as to close to 10^{-4} to improve the temporal response of the detector and cryocooler combination. The effective thermal capacity should be a system constraint, as it should be as close to a value as possible, but is instead used as a FoM in this research due to the inability to define a thermal constraint in the topology optimisation study in Solidworks. The last FoM is the mass of the FPA. These FoM can be used to compare designs to one another and must therefore be normalized accordingly, especially since the units of the FoM and their orders of of magnitude differ. The set of FoM to assess the performance of an FPA is listed below:

$$F_1 = \frac{m_0}{m} \tag{48}$$

$$F_2 = \frac{\kappa_{eff}}{\kappa_0} \tag{49}$$

$$F_3 = \frac{1}{1 + |\frac{C_{eff}}{10^{-4}} - 1|^{0.1}} \tag{50}$$

This set of FoM will describe the systems thermal performance and the mass reduction. A higher value for the first FoM will indicate a lower mass. A higher value for the second FoM will indicate a better effective thermal conductivity. A higher value for the second FoM will indicate that the system has an effective thermal conductivity which is closer to 10^{-4} $\frac{J}{K}$. The first two FoM are normalized so that further designs are compared to the original desing. The last FoM is not normalized but described by a function which gives the distance to the desired value. Assuming a value lower or higher than the target will deviate the FoM from 1, indicating distance to the preferred value. The penalty factor of 0.1 in the exponent of the absolute value has been arbitrarily determined to flatten out the response of deviations around the desired effective thermal capacity. This figure of merit is an indication of the importance of the thermal capacity and is in no manner optimal. The above defined FoM only consider physical system characteristics, but no practical considerations. A good measure to consider is average temperature of the detector array, which is in essence the quantity one would prefer to keep nominal. The average detector area temperature is however not considered as a FoM as it is an emergent property, resulting from a combination of the systems conductivity and capacity. The average detector temperature is not a system characteristic and is therefore not used as an FoM. Nonetheless it will be considered in the verification of the FPA's thermal performance in COMSOL as a metric to verify whether operational requirements are met.

4.3 Objective Function

All objective functions that Solidworks offers have been treated in section 3; their capabilities and limitations have been identified and will be considered when choosing the objective function best fit to optimising an FPA.

Considering that all objective functions are only relevant to optimisation with regards to mechanical considerations, the objective functions will be valued accordingly. The boundary conditions and constraints as mentioned in section 4.2 are what dictate which objective function is most relevant to an FPA. As an immediate consequences of the constraints, a displacement constraint is irrelevant to the optimisation of an FPA. The only deformation of the FPA will occur during the launch, where the position or orientation of the detector array is irrelevant. Naturally, one does not want the detector array to deform too severely that it may interfere with other equipment, but considering the fact that the FPA will be severely simplified, this will be neglected. This lack of displacement constraint therefore rules out the use of the minimise displacement objective function.

By default, this also regards the minimise displacement constraint in combination with the mass minimisation objective function as irrelevant. Additionally the minimise mass objective function

paired with a greater than frequency constraint will yield a design which is unusable, rendering this combination also unfit. The minimise mass objective function can however be employed with the relevant manufacturing constraints that consider a minimal member thickness or a preserved area, but that notion contradicts the objective function of minimising the mass. The von Mises stress constraint produced an inherently connected result and is relevant for an FPA. This optimisation however taxes the hardware significantly and is therefore unusable in this research. Additionally, the constraint must be active for the objective function to produce an inherently connected result, something which cannot be guaranteed with the boundary conditions of an FPA. The mass minimisation objective function can therefore not be used to optimise an FPA in Solidworks.

It is almost by default that the BSWR objective function is therefore chosen to be utilised in the topology optimisation of an FPA. Nonetheless, this objective function is not just the only one which is relevant, but it also displays significant strengths to optimise an FPA. The first being the inherent coherency of the structure that is created in the topology optimisation as seen in the figures in figure 29. The second being the advantage the objective function has when considering the eigenfrequencies, as the stiffness is directly related to the eigenfrequencies, this property is inherently considered. For the above reasons, the best stiffness to weight ratio objective function has been chosen over the minimise displacement and minimise mass objective functions to topology optimise the FPA, mainly due to its trustworthiness in yielding a coherent result and the lack of relevance of displacement constraints for an FPA.

4.4 Assumptions

Developing a CAD model which completely represents an FPA such as mounting points, material transitions and wiring is outside of the scope of this research, therefore, the CAD model is simplified. To also further simplify the simulation and modeling of an FPA, some assumptions are made, these are as follows:

- There will be no convection present in the FEM analysis due to the FPA being operated in space.
- There will be no radiation present in the FEM analysis considering the negligible amounts of radiation emitted by the parts at 50mK.
- The microvibrations that pass through the aramid chords are assumed to be a thermal load to be grouped with the thermal gradient along the chord.
- There will be no magnetic fields present in the thermal model as they are negligible and to avoid overcomplicating the system
- The thermal model will not consider thermal contact resistance as it is not relevant to the optimisation or performance of the CAD model which will be optimised
- The heat load will be time independent to be able to have a controlled environment to check thermal performance
- The thermal conductivity and thermal capacity of the material used will be a function of temperature as described in section 4.1.3
- The mechanical properties are assumed to be constant as they are not able to change in the topology optimisation setup in Solidworks either
- The thermal strap will have a set set temperature and not a duty cycle so as to remove the time dependence.

- Cosmic rays incident on the detector array are neglected
- The material used is assumed to be a perfectly homogeneous material
- Ambient temperature is irrelevant considering stationarity of the simulation
- All not participating faces, those without thermal boundary conditions, are considered thermally insulated

Some of the above assumptions are accurate to an actual FPA, for example the lack of convection and the dependence of the material properties on temperature. Other assumptions on the other hand are meant to simplify the simulation and case study to avoid making the system too complex, an example is the time independence of the heat load and cooler duty cycle. The above assumptions are mainly based on relevant physics but do not contain simplifications made to an FPA or limitations of the modeling software used; these will be discussed in the next section.

4.5 CAD model

If the model that is simulated is too complex, i.e. containing too many fixed, retained or input faces, the computing time rises exponentially and the essence of the optimisation is lost: one can no longer ascertain which parameters are important. There are certain boundary conditions and inputs that are relevant to an FPA which must be incorporated to understand how they influence the optimisation process. The full scope of connections, fixtures and geometrical details is neglected, instead a simplified geometry is created in which only the crucial aspects of an FPA are retained. The aspects of an FPA that are kept and overtly simplified are:

- Detector array
- Aramid suspension connections
- Thermal strap

The detector array (DA) in X-IFU a hexagon [14], is now assumed to be a square of dimensions 25x25mm. The aramid suspensions would usually have three times three chords which are unified into a single connection point; implicating that a heat load would go through a total of nine chords. The simplified aramid suspension connection is now a circle of diameter 8mm, where there used to be nine, there are now three, called S1, S2 and S3. Lastly, the thermal strap (TS) is represented as a circle of diameter 16mm located directly underneath the detector array. All of the above simplifications are represented in the below figure showcasing the CAD model to be used as an FPA.

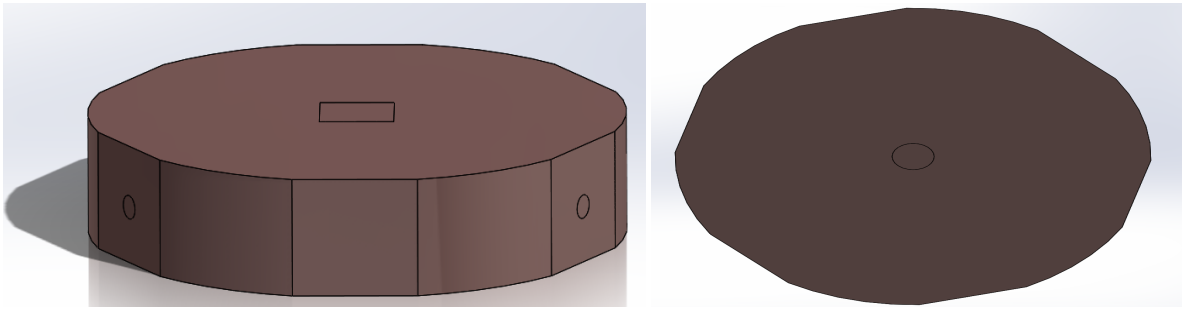

(a) ISO view. (b) Bottom view.

Figure 15: showing the simplified CAD model with the detector array, aramid suspensions connections and the thermal strap.

The CAD model as seen in the figure above is subject to the inputs and boundary conditions as seen in the table below.

Table 2: Showing all inputs of the CAD model.

Area	QSL(Ax. - Lat.) [g]	Heat input [nW]	Temperature [mK]	Mechanical constraint
Domain	60		-	-
S1	-	300	-	Fixed
S2	-	300	-	Fixed
S3	-	300	-	Fixed
DA	-	20	-	-
TS	-	-	50	-

The aramid suspensions connections are fully fixed in the CAD model, which is not a realistic scenario, as these aramid connection points still have three rotational degrees of freedom in an FPA. Considering that this setting is not available in Solidworks, the aramid suspension connections are said to be fully fixed.

5 Optimisation Routine

The methods to topology optimise an FPA, together with the relevant background information, have been identified, and must now be applied to an FPA. This section will consider the steps required to optimise an FPA, and the caveats that these steps bring with them. The optimisation routine follows the steps as seen in figure 3, in which inputs must first be defined, an FEA is done, and consequently the model is topology optimised and verified. The optimisation routine is performed by firstly topology optimising the model in Solidworks, after which it is exported and verified in COMSOL for its thermal and mechanical properties.

5.1 Inputs and Boundary Conditions

The first step in the routine is considering the relevant material inputs, boundary conditions and applied loads in the model. The material choice for a T0 FPA housing is copper. The material properties of copper as defined in Solidworks can be found in appendix J. Important to note is that the material properties as specified in Solidworks do not match the material properties mentioned in COMSOL. However, COMSOL allows for one to edit the material properties, so that one can match the material properties from Solidworks. This possible mismatch in material properties can lead to a false verification of the design in later steps. Further boundary conditions include the fixed constraints on the suspension connection points. As previously touched upon, these areas are fixed as this is the only constraint available in Solidworks. In COMSOL the user is able to define the degrees of freedom. The last mechanical boundary condition is the QSL, which is applied as a gravity load of 60 times the gravity. In Solidworks, one can define the direction in which the gravity acts, where usually it acts 'downwards', depending on the reference axes, but can also be defined by other planes. As mentioned in section 4.2, the FPA must be able to withstand a lateral and axial QSL, these are however not applied at the same time and are considered as separate load cases. These separate load cases can also be defined in Solidworks. Solidworks consequently considers both load cases in the simulation and topology optimisation will consider the effects of both load cases. For all intents and purposes, this does not make a difference in the optimisation routine and will therefore not be considered in the model. The boundary conditions that will be applied to the exported model in COMSOL will be discussed later, as the exporting process is of relevance to these boundary conditions.

5.2 Meshing

Once all inputs and boundary conditions have been defined, a mesh must be defined for the model with which to topology optimise the model. As seen in section 3.4.2, the finer the mesh, the more coherent the results appear to become. Especially when considering the von Mises stress constraint, which is a mesh dependent constraint, as large mesh element can cause stress singularities. Therefore, for von Mises stress constraints, a fine mesh must be chosen, at the expense of computing time. In Solidworks offers the option for a draft or high quality mesh; choosing the draft quality mesh will create larger elements and attribute less detail to the model, whilst choosing the high quality mesh is especially meant for the stress constraint and will improve accuracy but also increase computational time.

The purpose of this research is not to produce an optimised FPA, but rather discuss the details of optimising an FPA. Therefore, this meshing section is only relevant in indicating the dependence of the topology optimisation on the mesh of the model. This section will not detail or elaborate on the precise effects of how changing mesh density will affect the results, but will rather highlight the importance of a mesh study. A mesh analysis will however be performed for the verification of the final result to indicate the trustworthiness of the optimised result.

The test cases for the mass minimisation objective function with the displacement constraint as seen in section 3.4.2 gave an indication of the evolution of compute time as the mesh size decreased. The number of iterations and time taken to converge can be seen in appendix K, but showed that a mesh size of 0.5mm was too small as the runtime was exceeded. Considering both runtime and ease of exportation and handle-ability in COMSOL, a mesh size of 3mm was considered for the FPA, where the growth factor was left unchanged at 1.4. A smaller mesh size resulted in the core memory capacity being exceeded. Again, this step is also applicable when verifying the result in COMSOL, but will, as with the boundary conditions, be discussed in a later section.

5.3 Topology Optimisation Routine

In the optimisation step, the appropriate objective function is selected. As mentioned in section 4.3, the Best Stiffness to Weight Ratio was selected as the objective function with which to optimise the FPA. Applied as constraints are the following:

- Volume constraint = 75% of mass is removed
- Frequency constraint > 200Hz
- von Mises stress constraint <80% of original model von Mises stress

The von Mises stress should normally be considered as it is a constraint on the FPA, but as mentioned in section 3.4.3, will not be considered in the actual optimisation. The selection menu of the objective functions can be found in appendix K. optimisation using only the objective function and constrains will remove essential details in an FPA. There is no control on what elements the optimisation must retain, and can therefore remove essential areas in an FPA such as the detector area and the thermal strap. For this reason, the DA and TS areas in CAD are preserved using the preserved region function in Solidworks. The menu for this function is seen in appendix L. One is able to define the thickness of the preserved region, which extrudes the selected area. This option allows for the DA and TS to be preserved in the topology optimisation routine. Automatically preserved regions are faces which are selected as being fixed or as having an input boundary load, excluding gravity load. Adding preserved regions in Solidworks however has its caveats, considering that one imposes a lower mass constraint limit as one preserves a certain volume of elements. This means that in some cases, for example, one is unable to remove 90% of the mass as at least 10% of the mass kept is defined as a preserved region. The path between the DA and TS was conserved by defining the thickness of the preserved area as 20mm, both spanning halfway through the design. Secondly, to enforce symmetry in the design, one is able to add symmetry planes, these however only operate in halves, quarters and eighths.

Defining the objective function, constraints and other manufacturing constraints completes the set up required to optimise an FPA. During optimisation,the value of the objective function and the constraints are shown and the values can be tracked to confirm convergence. When the aforementioned values have converged, or the maximum number of iterations has been reached, the optimisation stops and the result is shown. The result of the topology optimisation as described above is shown below.

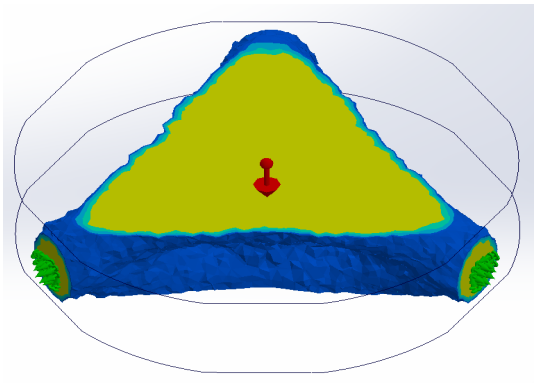

(a) FPA ISO view.

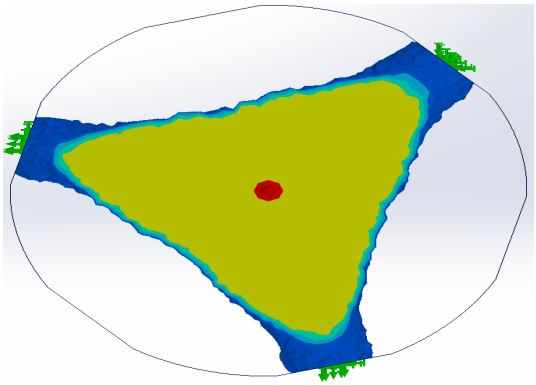

(b) FPA top view.

(c) FPA side view.

Figure 16: showing the topology optimised FPA from different perspectives.

The figure above shows the optimised FPA, in which the detector area, the thermal strap and all aramid connection points have been retained. The final mass of the resulting geometry is 2.3416kg. The first eigenfrequency of the model is 2073.3Hz. The convergence of the objective function and constraints can be seen in the figures below.

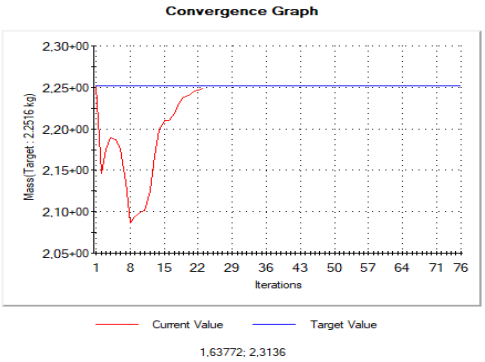

(a) Mass convergence.

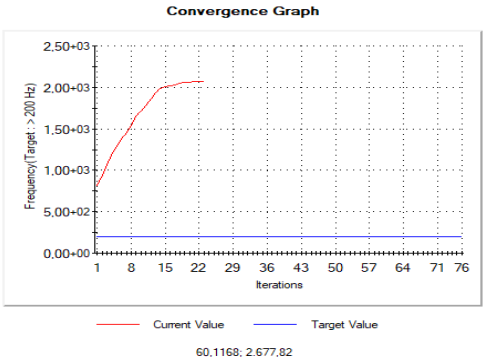

(b) Frequency convergence.

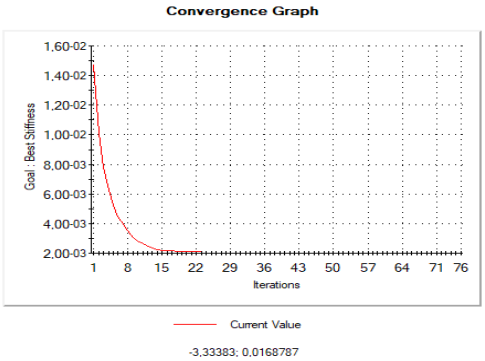

(c) Stiffness to weight ratio convergence.

Figure 17: showing the convergence graphs for the topology optimised FPA.

As evident from the figures above, the values for the objective function and constraints have converged. The convergence graph as seen in figure 20a shows a target value, which is the volume constraint defined beforehand. The result in figure 29b shows yellow and blue coloured elements; the colour of the elements depends on the relative density. As mentioned prior to this section, Solidworks shows elements with relative densities greater than 0.3. One is however able to select what relative densities are shown by adjusting the mass slider, the menu for which is shown in appendix M. Having the slider on the far left will show all elements and give the full mass of the system; having the slider on the far right will show only elements with full relative density. The default setting gives the elements whose masses add up to the volume constraint defined earlier. The results shown in figures 29a through 16c were taken with the mass slider at the default position.

5.4 Exporting

The topology optimised model is subsequently exported from Solidworks into COMSOL for a verification of the thermal and mechanical performance. To export the mesh, it must be smoothed. The menu for this function is shown in appendix M. Chunks seen in the unsmoothed model arre smoothed over and will be removed. One can see the difference between the rough and smoothed models in the figures below:

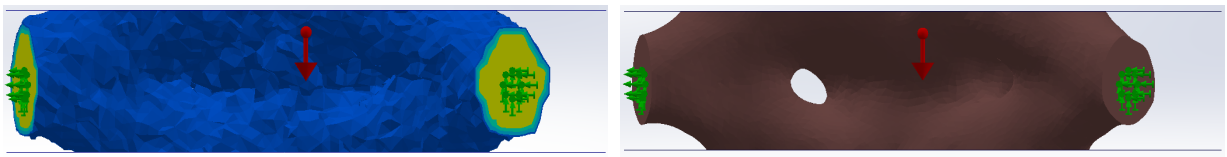

(a) FPA mesh side view. (b) FPA smoothed side view.

Figure 18: showing the difference between the coarse mesh and the smoothed mesh for the resulting optimised FPA geometry.

A smooth mesh is required for exportation. The function to export the mesh has limitations, the quality of the exported mesh is dependent on the method employed within the exporting menu. The method which was found to work was to export the model as an STL file, subsequently repairing the STL file in an online file repair service and then importing the repaired STL file as a solid or surface body in Solidworks. The geometry was then able to be imported into COMSOL for verification.

5.5 Verification and Analysis

Importing the file from Solidworks into COMSOL causes issues with intersecting elements that have badly transferred. The imported geometry must therefore first be cleaned up in COMSOL using a multitude of filters and clean-up operations. The cleaned up geometry can subsequently be used to define the inputs, where individual mesh faces must be selected as named selections as these geometrical details have been lost in the transfer between Solidworks and COMSOL. An example of this loss of detail is found in the aramid suspension points. These points were defined as circles in Solidworks and had transformed into a hexagon after the importation in COMSOL.

The default copper chosen in COMSOL has different material properties than those defined in Solidworks, and are therefore adjusted. The thermal conductivity and capacity are adjusted using the equations from section 4.1.3, the menus for this can be found in appendix N. It was found that for small temperature changes, defining the thermal conductivity of the material caused issues with the model which resulted in incoherent results. The thermal conductivity was therefore defined as $2.4\frac{W}{m \cdot K}$, as dictated by $(30/0.634) \cdot 0.05$. The boundary conditions have been previously described in section 4.2 and are applied to the detector area, thermal strap and suspension points. It is crucial that the 'Boundary Heat Source' function is used instead of 'Heat Flux', as using the latter will cause the simulation to fail. A mesh clean-up operation is required in COMSOL to run the simulation. The static study is run and the results can be analysed for its performance. The figure below shows the temperature distribution of the topology optimised FPA.

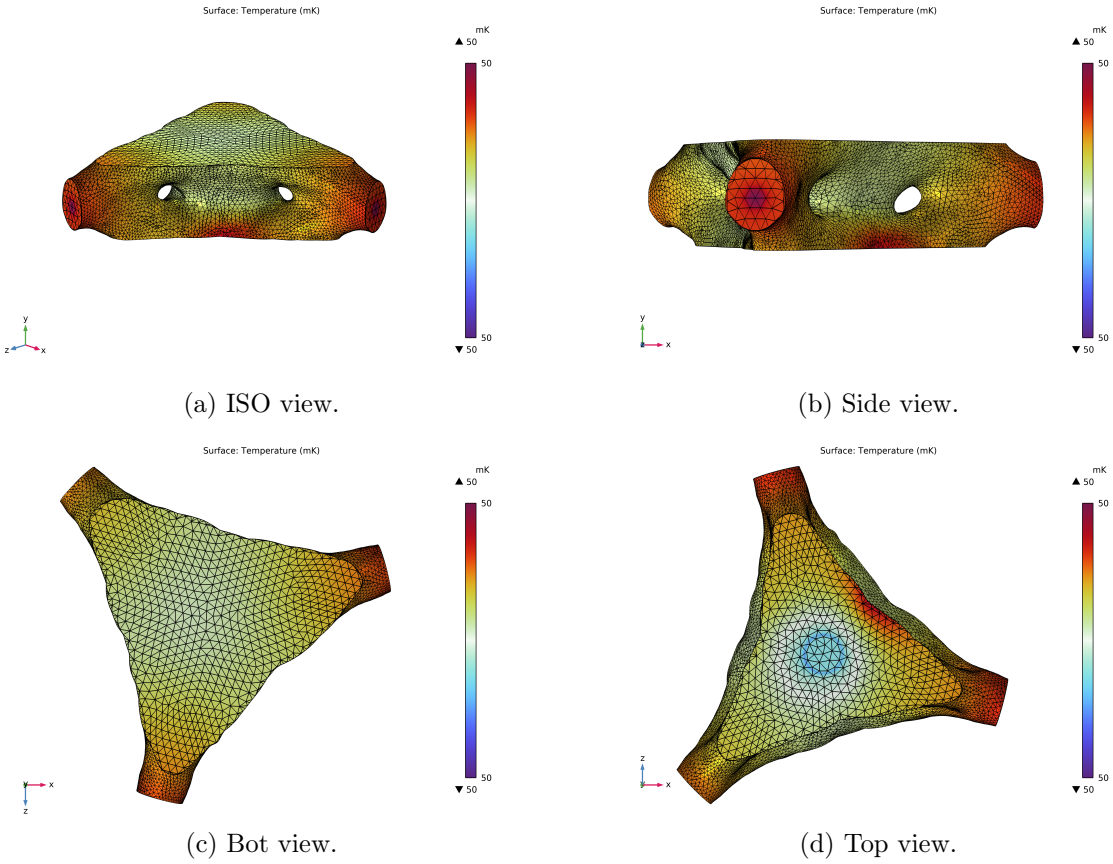

(a) ISO view.

(b) Side view.

(c) Bot view.

(d) Top view.

Figure 19: showing the different views of the temperature distribution in the topology optimised FPA.

The figures above show a clear temperature distribution along the FPA, where the aramid suspension connection points have heated the most: 0.01601mK higher than 50mK. The average detector area temperature is 50.0009mK. The seen temperature distribution raises some questions about the validity of the simulation. The locality of the heated elements at the bottom face of the FPA is unusual, as there is no heat load applied to that section. Additionally, this localised heating is also asymmetrical. For the simulations using the unoptimised FPA model, the reader is referred to appendix O. The other relevant data acquired from the verification of the FPA have been summarised in the table below:

Table 3: showing the relevant measured quantities for the optimised FPA

Quantity	Mass[kg]	Avg. Temp. DA [mK]	Frequency [Hz]	max. vM stress [MPa]	F_1	F_2	F_3
Value	2.341	0.50009	X	25.2	3.84	0.155	0.524

COMSOL was unable to calculate the eigenfrequency of the topology optimised result, therefore the value is omitted from the table above. The mass has improved by approximately 75%, the thermal conductivity worsened by 84.5% and the thermal capacity has approached the 10^{-4} value by approximately 30%. Although the thermal conductivity worsened by a significant amount, the average temperature of the detector array has increased by only 0.0006mK.

5.6 Mesh Analysis

To verify the accuracy of the simulation results in the previous section, a mesh analysis was performed where the mesh size was decreased and the sensitivity of the quantities in table 3 were measured. The mesh analysis decreased the mesh size from 0.0792m to 0.00317m. The data for the mesh analysis is shown in the table below.

Table 4: mesh size decrease, showing the relevant values as the maximum element size is decreased.

Mesh size	Mass[kg]	Avg. Temp[K]	Max v.M. Stress[MPa]	F_1	F_2	F_3	Maximum element size[m]
Extremely coarse	2.341	0.050006	11.1	3.84	0.155	0.524	0.0792
Extra coarse	2.341	0.050006	13.9	3.84	0.155	0.524	0.0475
Coarser	2.341	0.050006	20.9	3.84	0.155	0.524	0.031
Coarse	2.341	0.050006	22.9	3.84	0.155	0.524	0.0237
Normal	2.341	0.050006	26.1	3.84	0.155	0.524	0.0158
Fine	2.341	0.050006	32.4	3.84	0.155	0.524	0.0127
Finer	2.341	0.050006	44.7	3.84	0.155	0.524	0.00871
Extra fine	2.341	0.050006	31.7	3.84	0.155	0.524	0.00554
Extremely fine	2.341	0.050006	35	3.84	0.155	0.524	0.00317

It is evident from the table above that almost all relevant figures remain constant as the mesh size is altered. The maximum von Mises stress is the only value dependent on the mesh size. The location of the maximum von Mises stress was observed to consistently be located in the aramid suspension connection points. The fixed areas were defined as being hexagonal areas in the COMSOL simulation, rather than the original circles, causing sharp corners in the mesh. These sharp corners are primarily responsible for the stress singularities. The value of the maximum von Mises stress has not converged as the mesh size was decreased, but seemed to increase as the mesh size was reduced, and subsequently decrease. Further reducing the mesh size led to time outs in the run time of the simulation. To further investigate the effect of mesh size on the maximum von Mises stress, the mesh of the aramid suspension connection points were further refined using a local refinement, as a specified size for these elements could not be defined in COMSOL. The area surrounding the connection points and subsequently only the connection points were refined. The different mesh methods are shown in the figure below.

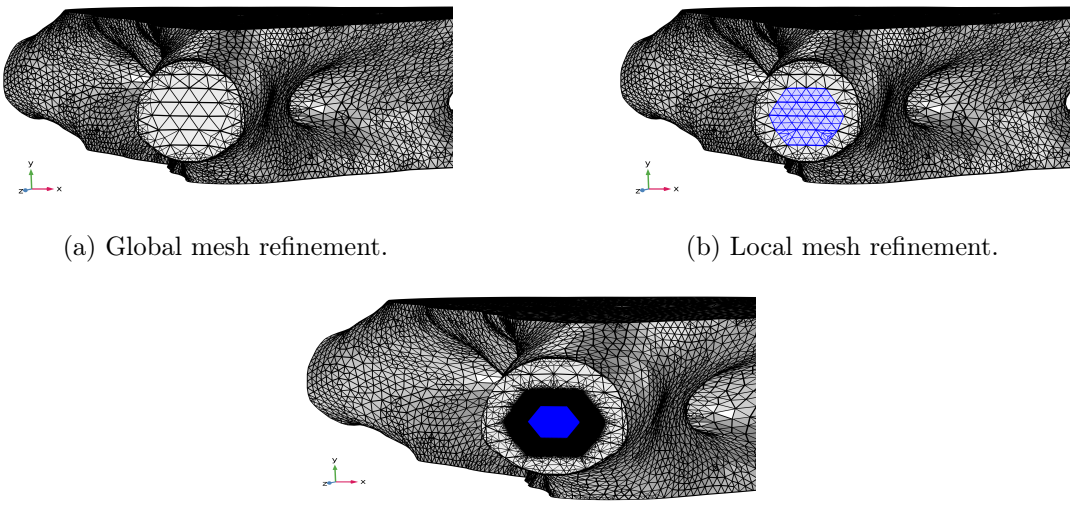

(a) Global mesh refinement.

(b) Local mesh refinement.

(c) Additional local mesh refinement.

Figure 20: showing the different methods of refining the mesh of the optimised FPA.

The results of the local mesh refinement are shown in the table below. The amount of refinements was limited by the run time time out due to lack of computing resources.

Table 5: mesh refinement showing the relevant values as the mesh is locally refined.

Mesh refinements	Mass[kg]	Avg. Temp[K]	Max v.M. Stress[MPa]	F1	F2	F3
1	2.341	0.050006	22.3	3.84	0.155	0.524
2	2.341	0.050006	35	3.84	0.155	0.524
3	2.341	0.050006	53.8	3.84	0.155	0.524
4	2.341	0.050006	83.8	3.84	0.155	0.524
5	2.341	0.050006	131	3.84	0.155	0.524
6	2.341	0.050006	170	3.84	0.155	0.524

The table above shows that, whilst the other values remain constant, the maximum von Mises stress significantly increases as the mesh is locally refined. The highest values for the von Mises stress were observed to be in the corners of the hexagonal faces which describe the aramid suspension points. The reason that the maximum von Mises stress increases as the mesh size is decreased locally is suspected to be due to the poorly defined fixed area, leading to high concentrations of stress around sharp geometrical definitions. Nonetheless, the other values relevant for an FPA were found to be consistent throughout the mesh analysis.

This section aimed to highlight the important steps in the process of optimising an FPA. Important in this process are the consistency of boundary conditions and material properties between the optimisation and verification software, the mesh size and the manner of exporting the optimised geometry. It has been shown that COMSOL Multiphysics is not able to consistently incorporate important physical properties relevant to an FPA. Examples are the inability to incorporate the dependence of the thermal conductivity on the temperature at low temperatures,

wrongly interpreting a Dirichlet boundary condition when low heat loads are applied to the system and an inability to calculate the eigenfrequency of the optimised geometry. Nonetheless, the optimised FPA has been verified in COMSOL and the FoM calculated to assess the performance of the topology optimised result. Lastly, a mesh analysis in COMSOL showed the dependence of the von Mises stress on the local mesh size. Only the von Mises stress was influenced as the mesh size was reduced, and to such an extent that it is suspected that the shape of the fixed area introduced small corner elements that served as stress singularities. To summarise, the process of optimising an FPA and verifying the result is chiefly hindered by the fact that one has to export the result from Solidworks into COMSOL and that geometrical details are lost as a result.

6 Discussion

The scope of this research is broad. To narrow down this scope, the research has focussed on the topology optimisation feature in Solidworks and has used a simplified FPA. The limited functionality of Solidworks combined with the simplifications may affect the validity of the results and must therefore be discussed. The first aspect whose effects will be considered will be the consequences of the softwares used and the validity of the boundary conditions. The second aspect discusses the implications of the objective function, optimisation solver and the figures of merit. Lastly, some aspects to topology optimisation still have to be explored. These will be elaborated upon in a section detailing recommendations and further research.

6.1 Softwares and Boundary conditions

It is important to discuss the extent of the influence the chosen software and boundary conditions have on the topology optimisation of an FPA. There are several limitations that have been identified throughout this research and will be treated below.

The aramid suspension connections are fixed geometries with no free DoF. This fixing adds an artificial stiffness to the FPA. The model in Solidworks therefore has an artificially higher frequency, which influences the optimisation process for a frequency constraint. The artificially added stiffness may result in an optimised geometry which, with realistic boundary conditions, does not meet the eigenfrequency requirements. Measures such as safety and design factors can be employed to account for this, but require knowledge of the quantity of the added stiffness to the system. The second issue concerning the eigenfrequency, is that its calculations performed for the base model of the FPA showed different eigenfrequencies in COMSOL and in Solidworks. The results of which are found in appendix O. This mismatch in eigenfrequencies between Solidworks and COMSOL strains to what extent the results acquired in Solidworks are accurate. The combination of the added artificial stiffness and the inherent mismatch in eigenfrequencies between softwares strengthens the necessity of validation of the results. However, within this research, the value for the eigenfrequency of the optimised geometry could not be verified in COMSOL. Whether the results meets the frequency constraint thus remains uncertain. A mesh analysis to confirm the behaviour of the eigenfrequency has not been conducted, but could serve as a basis for identifying the error between Solidworks and COMSOL. Additionally, the von Mises stress calculations also differed for the unoptimised model. The COMSOL simulation showed a maximum von Mises stress higher than that of Solidworks. For this mismatch, a mesh study to identify the error between Solidworks and COMSOL is also recommended. In a topology optimisation process where the von Mises stress is defined as a constraint, understanding the mismatch in stresses between Solidworks and COMSOL is important.

Secondly, the simulation was assumed to be time independent to simplify the verification of the thermal performance. In a realistic simulation, the applied heat loads vary with time. Similarly, the cryocooler operates on a duty cycle, periodically removing heat. Knowing the temporal variation of these heat loads is important in accurately assessing the effect of the thermal capacity of the optimised geometry. Additionally, topology optimisation problems become more complex as a time dependence is introduced. Firstly, because a transient simulation must be solved each iteration step, and secondly because the sensitivity analysis will include the temporal

derivative. A study on the effect of effective thermal capacity on the FPA performance should include transient responses in the topology optimisation routine.

Lastly, the validity of the results acquired in the COMSOL verification step are to be considered. The temperature distribution as seen in 19 shows an inexplicable asymmetry. The applied heat load is symmetric and cannot lead to such an assymetric temperature distribution. It was observed that using a heat load of two orders of magnitude larger, namely 10^{-5}W, a symmetric result was acquired. In figure 19, the TS area is also not uniformly at 50mK even though it has a Dirichlet boundary condition applied to it. The average temperature of the TS was measured to be 50.0006mK. This phenomenon was not observed when using a heat load of two orders of magnitude larger. Additionally, the thermal conductivity of the topology optimised FPA model was unable to be defined as temperature dependent, which was possible in the non optimised FPA model. Regardless, the temperature range is negligibly small so that the change in thermal conductivity is also negligible for these heat loads. The temperature dependence of the thermal conductivity only becomes relevant with higher heat loads. Defining the thermal capacity as a function of temperature however posed no issue with heat loads higher than those defined in section 4.2. Finally, the performed mesh analysis showed no indication of the dependence of the figures of merit on the mesh size. Only the maximum von Mises stress changed as the mesh size was decreased and local meshes were refined. As mentioned in section 5.6 concerning the mesh analysis, the dependence of the von Mises stress on the mesh size is speculated to be because of the manner in which the fixed area of the aramid suspension points is defined. In the verification step in COMSOL, these points are defined as the mesh faces forming a hexagon in the area where the original circular fixed area was. The corners of the hexagon are prone to stress concentrations. The use of faces with corners or sharp changes in geometry must therefore be avoided in use for fixed areas in mechanical interfaces to avoid an overt dependence on the mesh size.

6.2 Optimisation Solver, Objective Function and Figures of Merit

The primary point of uncertainty concerns which optimisation solver Solidworks employs. The optimisation solver used has significant implications on how the topology optimisation happens, and what factors influence the result. The primary assumption is that Solidworks employs either OC or MMA. The secondary assumption is that out of the two solvers, Solidworks is more likely to use OC, or an altered version of it. This assumption is based on the theory as described in section 2.1.1 and 2.1.2 concerning the handling of multiple constraints. This assumption is later used in explaining the functioning of the different objective functions which Solidworks offers, especially the mass minimisation objective function. In this section the rhetoric is used that the magnitude of the element volume term v_e is responsible for the incoherency observed when using the mass minimisation objective function. This rhetoric is valid under the assumption that OC is used, and that the 'steering' is dependent on the sign and magnitude of the ratio as defined in OC. If the assumption that OC is employed were to be wrong, the incoherencies observed can no longer be attributed to the direct dependence of the updating scheme on element volumes. Both MMA and OC use the sensitivity of the objective function, but MMA creates convex subproblems to approximate the Lagrangian behaviour and as a result is less sensitive to large element volumes. Further theoretical clarification would require knowledge on the values of the move limit variable, damping factors and asymptotes. These values are not clarified in

the documentation provided by Solidworks.

Filters are often applied in topology optimisation routines to smooth out mesh dependencies and remove chequerboard patterns and island creations. All modern topology optimisation routines employ a filter[5], but what filter Solidworks uses is also unknown. Nonetheless, the practical implications remain the same. A mesh size dependence is observed when using the mass minimisation objective function, but also the oscillatory behaviour of active constraints around the target value signifies an inability to handle multiple constraints well.

The used objective function, namely the best stiffness to weight ratio, is irrelevant to the thermal-mechanical optimisation of an FPA. The mechanical properties that are important in an FPA are considered as constraints in optimising an FPA: the maximum allowable von Mises stress and first eigenfrequency. These system characteristics are not optimised for, but rather optimised with. Attaining a higher value for the eigenfrequency than the constraint is not directly beneficial to the performance of an FPA. The BSWR objective function does however remove a specified amount of mass and ensures an inherent coherency of the design, but the value for which it optimises is irrelevant as long as the constraints are met. The minimise displacement objective function is also irrelevant to the relevant constraints of an FPA. The mass minimisation objective function is relevant for the optimisation of the mass of the FPA, but only in conjunction with constraints that are both relevant and ensure a connected design. Only active constraints influence the mass minimisation; inactive constraints fail to prevent all mass being removed. Even with an active frequency constraint, the SIMP method allows that ρ_{min} elements contribute to the global stiffness and eigenfrequency of the structure, artificially lowering the eigenfrequency. It is because the available constraints are either irrelevant, in the case of the nodal displacement, are not active in the case of von Mises stress, or can be 'bypassed' because of how the element densities are attributed that Solidworks offers no possibility in which the mass minimisation objective function can be utilised to optimise an FPA.

The sensitivity of the mass minimisation objective function to element volume was attributed to the optimisation solver used and how it utilised the sensitivity of the objective function. In contrast, the BSWR objective function was not shown to have this relatively strong dependence on the element volumes. The reason being that the sensitivity of the objective function is less dependent on the element volume. Additionally, because Solidworks employs the SIMP method which allows for ρ_{min} elements to contribute to the global stiffness, the mass minimisation objective function in combination with the frequency constraint yields results which are not are not usable. This is an important drawback in using the SIMP method which is not observed when using another method such as BESO[5]. The reliability of the mass minimisation objective function is therefore reliant on what optimisation solver is used, how the material is topologically described, but most importantly, whether the set of constraints includes an active constraint which forces the optimisation to yield an inherently connected result. In Solidworks, using the mass minimisation objective function with the three available constraints yields an inherently connected result, as the maximum displacement constraint is active and prevents the frequency constraint from being bypassed. Introducing the effective thermal conductivity and capacity as constraints will however not ensure an inherent connectivity. Both system characteristics are defined by a sum of individual element properties, making it irrespective of which elements can or cannot contribute to the sum. These constraints, whether active or inactive, will not yield an

inherently connected structure as any combination of randomly retained elements will allow for the constraint to be satisfied. A constraint being active therefore does not ensure an inherently connected result. The reason why the displacement constraint ensures connectivity is because of the tendency to minimise the total strain energy. The capacity does not benefit from forming a connected structure as it will not affect the sum of capacities. Considering the above, mass minimisation will only be useful as an objective function if used with an active constraint that ensures connectivity, but also with an optimisation solver that is less mesh dependent and is able to handle multiple constraints.

The FoM defined in section 4.2 are used in gauging the system performance. They were ascertained by identifying the relevant system characteristics that are not constrained but must be optimised for. The FoM concerning the improvement in the mass of the system is a good indication to what extent the mass has changed relative to the original mass. The second FoM concerning the improvement of the effective thermal conductivity of the system is also a straightforward indicator of performance. Because the effective thermal conductivity is denoted as a FoM, the notion is conceived that the higher this ratio, the better the performance of the FPA will be. However, the practical consideration must be taken into account that a certain value for the effective thermal conductivity is in fact good enough for the performance of the FPA. In section 4.1.2, the T0 housing resistance was assumed to be negligible compared to the strap resistance. This however introduces a constraint on the effective thermal conductivity of the system. For the thermo-electrical analogy to hold, the T0 conductivity must be higher than the conductivity of the thermal strap. As this consideration introduces a threshold value for the effective thermal conductivity of the system, the second FoM could also be compared to it. Whether the FoM for the effective thermal conductivity should be described as a ratio between the new and original value or how well it approximates the threshold value is dependent on the use case. Lastly, the third FoM is based on simplifications of the thermal system. It is assumed that the path of the cyrocooler to the T0 housing of the FPA is only interjected by the thermal strap. There are myriad unconsidered systems in the FPA which add both thermal resistance and capacitance, but are neglected in the analogy. Additionally, the heat loads incident on the system are not described in the thermal model. These heat loads are time dependent and placed at different locations in the circuit describing the thermal model. They influence the temporal response as they add disturbances to the control system. Only once the entire scope of resistances, capacitances and disturbances has been identified, can a target value for the effective thermal capacitance of the T0 housing accurately be determined. Lastly, the penalty factor of 0.1 introduced in the third FoM was chosen arbitrarily as to flatten out the response of the FoM to fluctuations of the thermal capacity. This value is not an optimal value based on analytical proof, but rather one chosen to showcase the concept. Altering this value will impose more or less importance on the thermal capacity of the system.

The COMSOL simulations of the optimized FPA indicated that whilst the decrease in the effective thermal capacity was significant, the increase in average detector area temperature was negligible. This raises the question to what extent the FoM of thermal conductivity is an accurate representation of the performance of the FPA. Important in this discussion is that the heat loads, that are representative for an FPA, are so low that they seem to influence the temperature distribution of the FPA insignificantly. So a large decrease in the thermal conductivity has a small effect on the negligible amount of heat loads present on the FPA. The same simulation was

performed on the optimised and unoptimised FPA with the heat loads two orders of magnitude higher and it showed that the average detector area temperature were 50.674mK and 50.638mK respectively, implying the obvious dependence of the detector array on the applied heat loads and thermal conductivity of the system. The FoM of thermal conductivity is therefore only considerably important in systems where the heat load is higher than that defined in an FPA. This statement is valid under the simplified version of this FPA, where a large amount of heat loads have been removed.

6.3 Further Research and Recommendations

This research has shown the possibilities of topology optimisation within Solidworks for an FPA. The parameter for which was optimised, the best stiffness to weight ratio, was however irrelevant to the FPA. It has been discussed that the minimise displacement objective function also does not optimise for a relevant system characteristic and that the mass minimisation objective function, although relevant, can only be meaningfully employed using constraints. Although the BSWR objective function allows for a combination of all constraints to be added, ensuring an FPA is able to meet the frequency and von Mises stress constraints, there is no thermal optimisation that can be performed in Solidworks. This section will detail how thermal behaviour can be considered in the topology optimisation process in Solidworks and which aspects to the optimisation of an FPA require further research.

To incorporate a certain control of thermal system characteristics, one can define a preserved area in Solidworks with a specified depth. If the detector array and thermal strap are underneath one another, a direct path between the detector array and the thermal strap can be defined. This direct path ensures that heat can flow more directly from the DA to the TS, presumingly lowering the equilibrium temperature of the DA. Additionally, one is able to define symmetry in the design to ensure there is no thermal gradient across the detector array. Lastly, minimum member thicknesses can be defined which also serve as thermal pathway to ensure heat flow. These concepts are left as suggestions based on the relevant physics and the possibilities supplied by Solidworks.

The above suggestions allow the user to somewhat consider thermal system characteristics in the optimisation process, but do not allow for optimisation of them. To optimise an FPA for its thermal properties, Solidworks is therefore a software unfit to do so. An FPA must therefore be optimised in COMSOL to consider the thermal properties. Additionally, the conversion from Solidworks to COMSOL is complicated, where mismatches in calculations have been shown, material properties are defined differently and that Solidworks has less options when it comes to mechanical interfaces and combinations of physics. These drawbacks are further emphasised by the difficulties of exporting a topology optimised result from Solidworks to COMSOL. It is therefore recommended that COMSOL is used to topology optimise an FPA.

This research has shown that through the use of FoM, the performance of an FPA can be assessed. The thermal system characteristics were used as FoM whereas the mechanical system characteristics were used as constraints. Although the effective thermal conductivity and capacity do represent the thermal performance of an FPA, they can also be defined as constraints. The effective thermal conductivity of the thermal strap should be negligible compared to the T0

housing, and the effective thermal capacity of the housing should exhibit a value in the same order of magnitude as the thermal resistance of the thermal strap. The only FoM that is left as a parameter to measure the FPA's performance, is the mass. If system characteristics can be posed as constraints, they can no longer be FoM. They do not describe the performance of the FPA but are rather a value to adhere to. In contrast, the emergent properties such as average detector temperature and the temperature gradient along the detector area are now relevant as FoM. One would be able to gauge system performance using these emergent FoM. Using these emergent FoM, one could study the FPA performance by changing the constraints to be more or less stringent.

The goal of the optimisation of an FPA is to optimise the mass and thermal and mechanical properties. In this research, the optimisation of the FPA has been regarded as minimising the mass, maximising thermal conductivity, and adhering to the imposed constraints. In this framework, either system characteristic can be used as the objective function, under the assumption that the topology optimisation process allows for consideration of thermal system characteristics. maximising the effective thermal conductivity of an FPA would require constraints on the volume, eigenfrequency, von Mises stress and effective thermal capacity. The topology optimisation would optimise for all system characteristics, but when the constraints are satisfied, only consider improving the thermal conductivity. Similarly, using mass minimisation as the objective function would require constraints on all of the aforementioned additional to the effective thermal conductivity. However, the framework this research considered is limited, as it supposes that the mechanical system characteristics are by definition constraints. The framework of this research does not consider that an FPA can also be optimised for a highest eigenfrequency, or lowest von Mises stress. It is dependent on the system requirements, which of these system characteristics is to be optimised for. Therefore, any system characteristic can be utilised as the objective function, with the other system characteristics posed as constraints. A combination of weighted system characteristics can also be defined as the objective function to optimise for several system characteristics simultaneously.

Using the effective thermal conductivity or capacity as constraints does not ensure usable results. Using them as objective functions will therefore also not ensure usable results. As an alternative to thermal conductivity, thermal optimisation is performed using the thermal compliance[6]. It is similar to the structural compliance formulation and also ensures an inherently connected structure. A similar objective function has not been found in literature for the effective thermal capacity and must therefore either be constructed or the system characteristic must be kept as a constraint. Furthermore, it is recommended that an objective function contains an internal energy to, in principle, ensure connectivity in the design. This internal energy can also be incorporated into a constraint, as seen in the displacement constraint. Further research is required on the objective functions to use to optimise for the eigenfrequency or maximum allowable von Mises stress.

If one were to use an objective function which would consider both mass and thermal compliance, the optimisation problem would become a multi-objective optimisation problem. This would require considering adding weights whose value would depend on the priorities of the user. These weights would introduce something called a Pareto front[33], which describes the behaviour of the objective function as one changes the weights of the design variables in the

objective function. A multi-objective function is more computationally heavy than a single objective optimisation problem. Additionally, the effects of the added weights must be investigated by creating a Pareto front to identify the optimal set of results. A multi-objective optimisation problem would also require consideration on whether the system characteristics are used in a linear superposition or in a different configuration. This also alters the Pareto front.

It must be stated again that although this research suggests that system characteristics should be employed as constraints or as an objective instead of as a FoM, these quantities are still useful in assessing emergent system properties. Previous sections have referred to several emergent properties which can be used as FoM, however, it is suggested that further research is required to identify more emergent properties that can be used as FoM.

This research has been conducted using Solidworks and the framework that has been created to optimise an FPA is built around the SIMP formulation and OC solver Solidworks uses. The practical considerations this research suggests are therefore a result of how Solidworks topology optimises and the limitations of its methodologies. Theory supports that the OC method is unable to handle multiple constraints well. The theory is supported by the oscillatory behaviour of the constraints, confirming the use of OC by Solidworks. The use of MMA or other solvers to handle optimisation problem formulations with multiple constraints is therefore recommended. Using different optimisation solvers or material distribution methods will yield different results and practical considerations. These different methods are available in COMSOL and it is suggested that further research investigates a multitude of aspects including, but not limited to: multiple constraint handling, element volume dependence and ρ_{min} element stiffness contributions. The reader is referred to [17] for an in-depth analysis of the performance of different solvers used in topology optimisation problems.

Lastly, it must be noted that topology optimisation yields results which are meant as indicators of an optimised design. As seen in section 3, many designs yield questionable material distributions. Topology optimisation is a tool to create designs which optimise a certain system characteristic, but are not meant to be copied and blindly used. Acquired geometry must be verified, and preferably even recreated using CAD software to ensure that the geometry is as the user wishes it to be.

7 Conclusion

This research aimed to investigate how topology optimisation can be used to optimise the mass and thermal-mechanical properties of an FPA. Firstly, the capabilities of topology optimisation in Solidworks were explored. Secondly, The relevant physical theories, boundary conditions and constraints were identified for an FPA, which were subsequently used to topology optimise an FPA and verify its performance in COMSOL.

A benchmark case was created to investigate the capabilities of topology optimisation in Solidworks. This showed that Solidworks offers only mechanical optimisation objective functions, of which the minimise displacement is irrelevant for the considered application. The mass minimisation objective function showed a significant dependence on the element volume and only produced inherently connected results with an active displacement constraint or an active von Mises stress constraint. The BSWR objective function produced inherently connected results which satisfied the constraints, but optimised for a maximum stiffness, which is also not relevant in this framework. Additionally, under the assumption that Solidworks uses the OC solver, the limitations of the solver were discussed and results showed a dependence on the element volumes and oscillatory behaviour of the constraints around the target value.

Through the results acquired by benchmarking the mass minimisation objective function, it was determined that the objective function is unreliable when used with constraints that are inactive or can be bypassed. The introduction of thermal constraints does not influence the reliability of the mass minimisation objective function as they do not ensure an inherently connected result. It was found that through the use of constraints which dictate an internal energy, such as the total strain energy, an inherently connected structure is ensured.

The relevant system characteristics for which to optimise were subsequently identified as being the effective thermal conductivity and capacity, the eigenfrequency and the maximum allowable von Mises stress. The framework of this research suggested that the mechanical system characteristics should be set as constraints and the thermal ones set as FoM. The limitations of the framework were discussed and it was concluded that all system characteristics are suitable for use as objective functions. The choice of objective function is case specific, but this research shows that using an objective function which, in princple, ensures an inherently connected result will yield a more reliable optimisation. The BSWR, thermal compliance and minimise displacement objective functions are examples which would yield reliable results, whereas mass minimisation or thermal conductivity maximisation would not.

Using the FoM and constraints, the topology optimised FPA had a 75% reduction in the mass, a 84.5% decrease of the effective thermal conductivity, and a relative improvement of 30% in the effective thermal capacity. The optimisation allowed for a substantial and controllable mass reduction, but no control over thermal system characteristics. Hence, the thermal conductivity has become poorer. However, the average detector area temperature increased by a negligible 0.0003K. The eigenfrequency of the system could not be verified in COMSOL and the maximum von Mises stress was too reliant on the mesh size that no converged value for it was determined.

Documenting this process highlighted the key issues with using Solidworks for topology op-

timisation and consequently using COMSOL for verification. Solidworks can only define a fixed geometry, adding uncertainty to the validity of the eigenfrequency of the system. Additionally, the export from Solidworks to COMSOL removes geometrical details which lead to difficulties in meshing the result in COMSOL. It is also for these practical limitations that use of Solidworks for topology optimisation is not recommended.

In summary, this research has demonstrated that the used framework for an FPA allows optimisation for its thermal-mechanical properties using topology optimisation in Solidworks. For a generalised framework, it is imperative that the system's constraints are identified in addition to the system characteristic used as the objective function. For reliable results that are inherently connected, an optimisation solver capable of handling multiple constraints and an objective function which ensures connectivity must be employed. Ultimately, this research concludes that whilst Solidworks offers a way to topology optimise an FPA for its mechanical properties, the full scope of the thermal-mechanical optimisation of a deeply cooled focal plane assembly using a robust solver, an objective function which incorporates an internal energy and the relevant constraints, is recommended to be performed using COMSOL Multiphysics.

8 References

[1] H. Azegami, *Shape Optimization Problems*. Springer Singapore, 2020.

[2] M. P. Bendsøe and N. Kikuchi, "Generating optimal topologies in structural design using a homogenization method," *Computer Methods in Applied Mechanics and Engineering*, vol. 71, p. 197–224, Nov. 1988.

[3] S. O. Bendsøe, M.P., *Topology Optimization : Theory, Methods, and Applications*. Springer, Berlin Heidelberg, 2004.

[4] A. Michell, "The limits of economy of material in frame-structures," *Philosophical Magazine*, vol. 8, no. 47, pp. 589–597, 1904.

[5] D. Yago, J. Cante, O. Lloberas-Valls, and J. Oliver, "Topology optimization methods for 3d structural problems: A comparative study," *Archives of Computational Methods in Engineering*, vol. 29, p. 1525–1567, Aug. 2021.

[6] Q. Meng, B. Xu, C. Huang, and G. Wang, "Lightweight topology optimization of thermal structures under compliance, stress and temperature constraints," *Journal of Thermal Stresses*, vol. 44, p. 1121–1149, Aug. 2021.

[7] X. Shen, H. Han, Y. Li, C. Yan, and D. Mu, "A topology optimization based design of space radiator for focal plane assemblies," *Energies*, vol. 14, p. 6252, Oct. 2021.

[8] S. D. Larsen, O. Sigmund, and J. P. Groen, "Optimal truss and frame design from projected homogenization-based topology optimization," *Structural and Multidisciplinary Optimization*, vol. 57, p. 1461–1474, Mar. 2018.

[9] J. Moreno, E. Vielba, A. Manjón, A. Motos, E. Vázquez, E. Rodríguez, D. Saez, M. Sengl, J. Fernández, G. Campos, D. Muñoz, M. Mas, A. Balado, G. Ramos, C. Cerruti, M. Pajas, I. Catalán, M. A. Alcacera, A. Valverde, P. Pflueger, and I. Vera, "Plato fpa. focal plane assembly of plato instrument," in *International Conference on Space Optics — ICSO 2018* (N. Karafolas, Z. Sodnik, and B. Cugny, eds.), p. 130, SPIE, July 2019.

[10] "X-ifu in a nutshell." Date Accessed: 03-06-2025, url = https://x-ifu.irap.omp.eu/en/x-ifu/x-ifu-in-anutshell.

[11] D. J. W. R. v. L. D. Jackson, B., "Fpa section of xifu srr design document," tech. rep., SRON, 2023.

[12] M. Eggens, "Possible configurations prima fpa," tech. rep., SRON, 2022.

[13] M. D. Lucia, P. D. Bo, E. D. Giorgi, T. Lari, C. Puglia, and F. Paolucci, "Transition edge sensors: Physics and applications," *arXiv preprint arXiv:2411.01968*, 2024.

[14] H. van Weers, "Dm fpa thermal simulation model," tech. rep., SRON, 8 2018.

[15] A. Parkinson and J. Balling, R.J.and Hedengren, *Optimization Methods for Engineering Design: Applications and Theory*, pp. 140–170. Brigham Young University, 2013.

[16] N. H. Kim, T. Dong, D. Weinberg, and J. Dalidd, "Generalized optimality criteria method for topology optimization," *Applied Sciences*, vol. 11, p. 3175, Apr. 2021.

[17] S. Rojas Labanda and M. Stolpe, "Benchmarking of optimization methods for topology optimization problems," 2014. 11th World Congress on Computational Mechanics, 5th European Conference on Computational Mechanics, 6th European Conference on Computational Fluid Dynamics ; Conference date: 20-07-2014 Through 25-07-2014.

[18] Y. W. Yin, L., "Optimality criteria method for topology optimization under multiple constraints," *Computers Structures*, 2001.

[19] K. Svanberg, "The method of moving asymptotes - a new method for structural optimization," *International Journal for Numerical Methods in Engineering*, 1987.

[20] M. Bendsøe, "Optimal shape as a material distribution problem," *Structural Optimization*, 1989.

[21] S. Help, *SIMP Method for Topology Optimization*, 2025.

[22] E. Andreassen, A. Clausen, M. Schevenels, B. S. Lazarov, and O. Sigmund, "Efficient topology optimization in matlab using 88 lines of code," *Structural and Multidisciplinary Optimization*, vol. 43, p. 1–16, Nov. 2010.

[23] J. Coors-Blankenship, "Myth dispelled: Topology optimization is not true generative design." https://www.ptc.com/en/blogs/corporate/myth-dispelled-topology-optimization-is-not-true-generative-design, 5 2019.

[24] D. D. B. T. L. A. Incropera, F.P., *Fundamentals of Heat and Mass Transfer*. John Wiley Sons, 2007.

[25] G. D. Robertson, A.F., "An electrical-analog method for transient heat flow analysis," *Journal of Research of the National Bureau of Standards*, 1958.

[26] F. Probell, *Matter and Methods at Low Temperatures*. Springer, 2007.

[27] E. D. N.J. Simon and R. Reed, "Properties of copper and copper alloys at cryogenic temperature," *NIST Monograph 177*, 1992.

[28] D. Mann, "Lng materials and fluids," *National Bureau of Standards, Cryogenics Division*, 1977.

[29] Arianespace, "Ariane 6 user's manual, issue 2 revision 0," 2021.

[30] Arianespace, "Vega-c user's manual, issue 0 revision 0," 2020.

[31] I. Y. W. M. Okawa, I., "Fundamentals of structural dynamics," 2007. Lecture note from Hokkaido University.

[32] T. Megson, *Aircraft Structures for Engineering Students*. Butterworth-Heinemann, 6th ed., 2016.

[33] K. Miettinen, *Nonlinear Multiobjective Optimization*, vol. 12 of *International Series in Operations Research Management Science*. Springer, 2012.

Appendix

A Convergence Graph

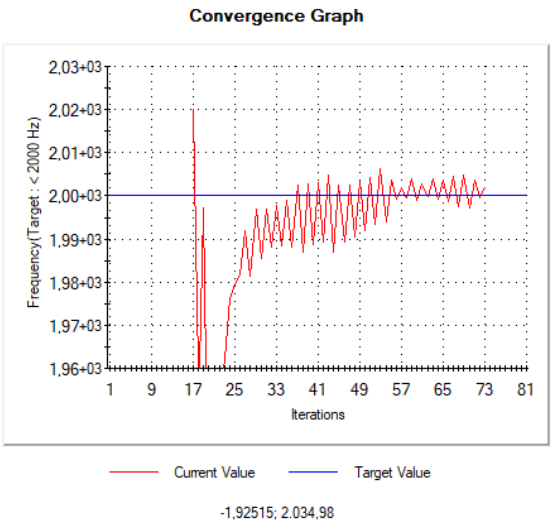

Figure 21: showing oscillatory behaviour of the design's eigenfrequency around the constraint value.

B BSWR Data

Mass percentage kept	100	80	60	40	20	10	5
Final Mass [kg]	0.356	0.29668	0.213393	0.15502	0.07937	0.0359	0.01238
BSWR	X	$1.78{\cdot}10^{-5}$	$9.31{\cdot}10^{-6}$	$5.83{\cdot}10^{-6}$	$4.50{\cdot}10^{-6}$	$4.26{\cdot}10^{-6}$	$2.6{\cdot}10^{-6}$
Total Strain Energy [J]	$8.444{\cdot}10^{-6}$	$3.05{\cdot}10^{-6}$	$1.594{\cdot}10^{-6}$	$1.003{\cdot}10^{-6}$	$1.066{\cdot}10^{-6}$	$1.039{\cdot}10^{-6}$	9.077cd

C Repetition proof

Iteration number	1	2	3	4	5	6	7	8	9	10
Mass [kg]	0.19006	0.19006	0.19006	0.19006	0.19006	0.19006	0.19006	0.19006	0.19006	0.19006
BSWR	$6.956{\cdot}10^{-6}$	$6.956{\cdot}10^{-6}$	$6.956{\cdot}10^{-6}$	$6.956{\cdot}10^{-6}$	$6.956{\cdot}10^{-6}$	$6.956{\cdot}10^{-6}$	$6.956{\cdot}10^{-6}$	$6.956{\cdot}10^{-6}$	$6.956{\cdot}10^{-6}$	$6.956{\cdot}10^{-6}$
Number of iterations	46	46	46	46	46	46	46	46	46	46
Time [minutes:seconds]	3:02	3:02	2:59	3:00	3:03	3:01	3:05	3:02	3:02	3:10

Iteration number	11	12	13	14	15	16	17	18	19	20
Mass [kg]	0.19006	0.19006	0.19006	0.19006	0.19006	0.19006	0.19006	0.19006	0.19006	0.19006
BSWR	$6.956{\cdot}10^{-6}$	$6.956{\cdot}10^{-6}$	$6.956{\cdot}10^{-6}$	$6.956{\cdot}10^{-6}$	$6.956{\cdot}10^{-6}$	$6.956{\cdot}10^{-6}$	$6.956{\cdot}10^{-6}$	$6.956{\cdot}10^{-6}$	$6.956{\cdot}10^{-6}$	$6.956{\cdot}10^{-6}$
Number of iterations	46	46	46	46	46	46	46	46	46	46
Time [minutes:seconds]	3:06	3:05	3:04	3:02	3:08	3:01	3:07	3:02	3:02	3:05

D ISO View BSWR

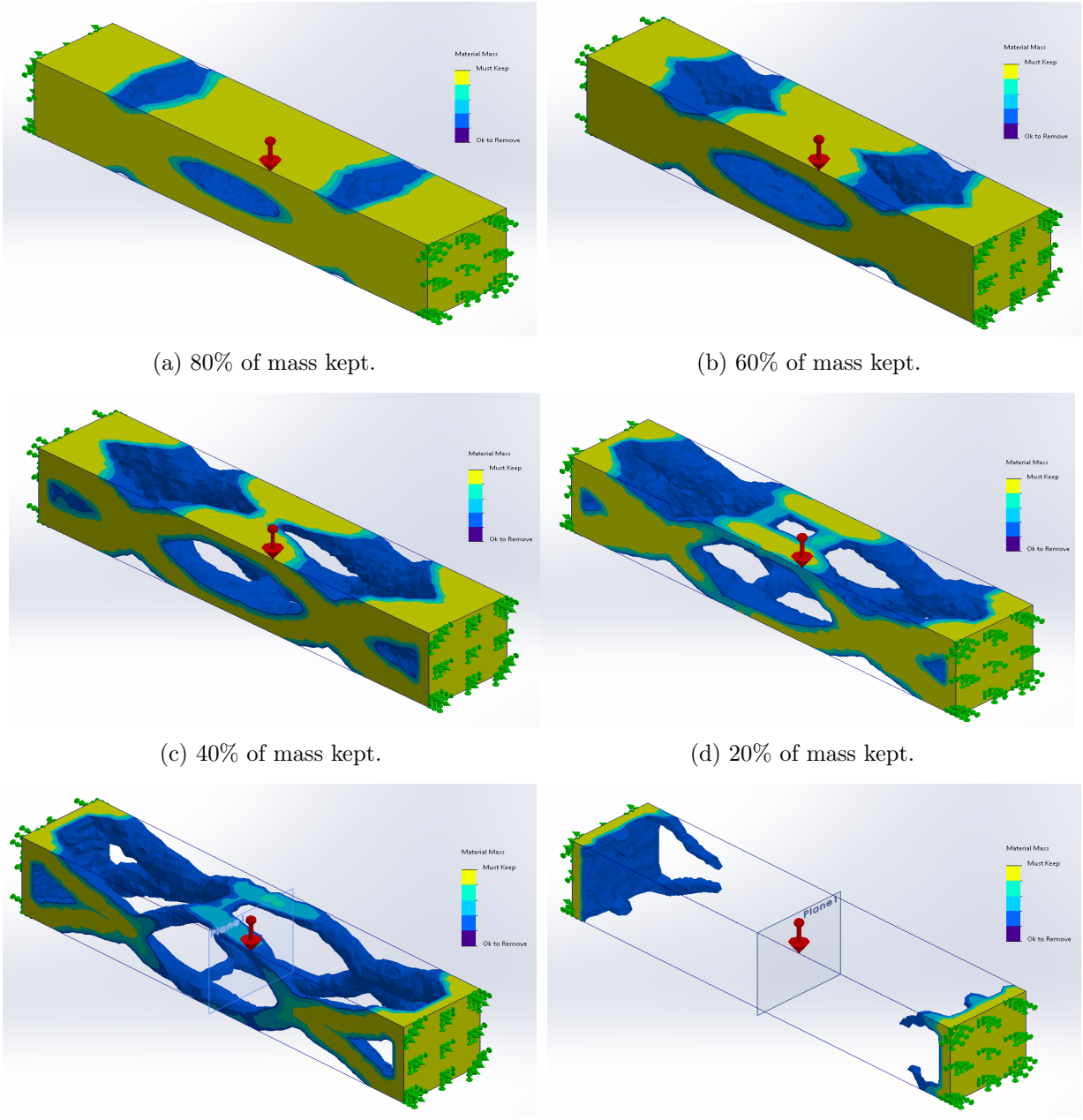

(a) 80% of mass kept.

(b) 60% of mass kept.

(c) 40% of mass kept.

(d) 20% of mass kept.

(e) 10% of mass kept.

(f) 5% of mass kept.

Figure 22: showing the ISO views of BSWR objective function results.

E minimise Displacement Data

Case	Static Study	1 Node active	2 Nodes active
Node 1 Displacement [mm]	$5.50{\cdot}10^{-4}$	$1.40{\cdot}10^{-6}$	$5.15{\cdot}10^{-7}$
Node 2 Displacement [mm]	$5.50{\cdot}10^{-4}$	$1.04{\cdot}10^{-2}$	$5.53{\cdot}10^{-7}$
Average Displacement [mm]	$3.25{\cdot}10^{-4}$	$3.14{\cdot}10^{-3}$	$2.83{\cdot}10^{-4}$

F Mode plots

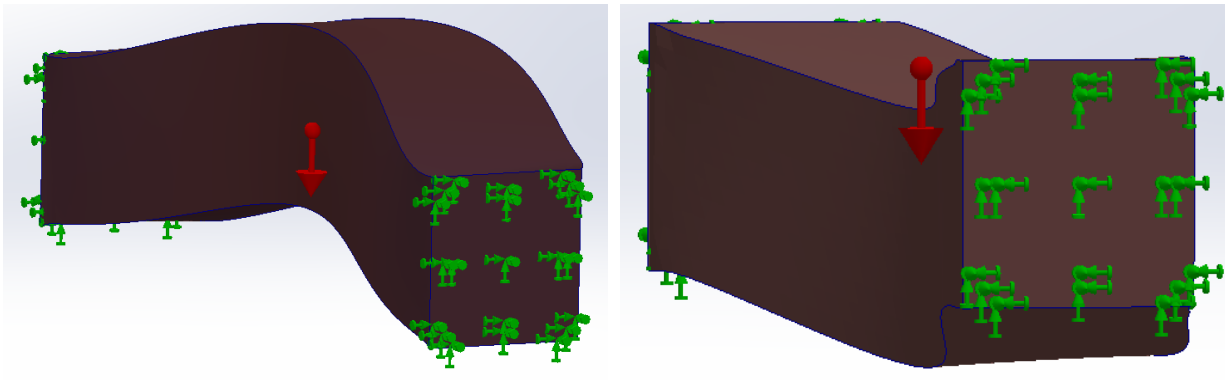

(a) Original Mode plot.

(b) Mode plot >4000Hz.

Figure 23: showing the mode plots for the original test case and the topology optimised case with a frequency constraint of >4000Hz.

G Mass minimisation Displacement Constraint data

Mesh Size [mm]	5	4	3	2	1	0.75
Node 1 Displacement [mm]	$3.95{\cdot}10^{-4}$	$1.50{\cdot}10^{-4}$	$6..45{\cdot}10^{-4}$	$2.26{\cdot}10^{-3}$	$4.63{\cdot}10^{-4}$	$5.45{\cdot}10^{-3}$
Node 2 Displacement [mm]	$7.86{\cdot}10^{-4}$	$1.50{\cdot}10^{-4}$	$1.54{\cdot}10^{-3}$	$7.847{\cdot}10^{-4}$	$1.35{\cdot}10^{-3}$	$4.39{\cdot}10^{-3}$
Mass [kg]	0.06842	0.05172	0.01995	0.01332	0.00897	0.00579

H BSWR Mesh Independence

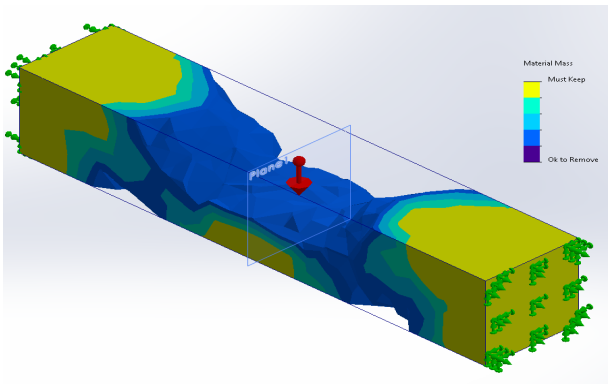

(a) 5mm.

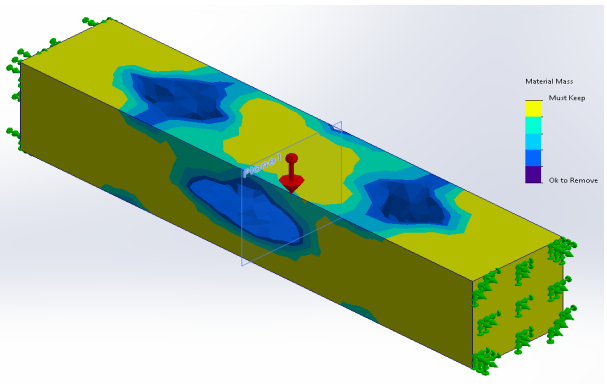

(b) 4mm.

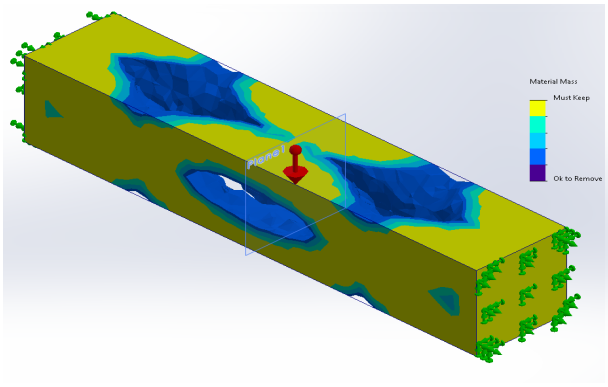

(c) 3mm.

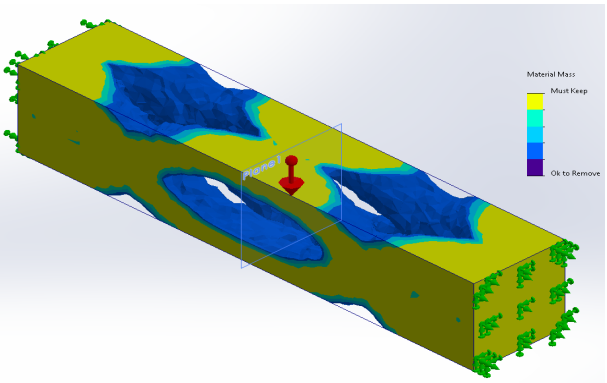

(d) 2mm.

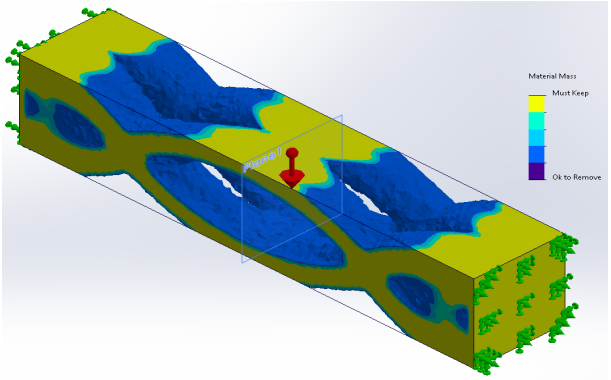

(e) 1mm.

Figure 24: showing the mesh dependence using the BSWR objective function.

I Effective Thermal Capacity Coefficients

n	A_n
1	$9.9434 \cdot 10^{-1}$
3	$4.7548 \cdot 10^{-2}$
5	$1.6314 \cdot 10^{-6}$
7	$9.4786 \cdot 10^{-8}$
9	$-1.3639 \cdot 10^{-10}$
11	$5.3898 \cdot 10^{-14}$

J Material Properties

Property	Value	Units
Elastic Modulus	1.1e+11	N/m^2
Poisson's Ratio	0.37	N/A
Shear Modulus	4e+10	N/m^2
Mass Density	8900	kg/m^3
Tensile Strength	394380000	N/m^2
Compressive Strength		N/m^2
Yield Strength	258646000	N/m^2
Thermal Expansion Coefficient	2.4e-05	/K
Thermal Conductivity	390	W/(m-K)
Specific Heat	390	J/(kg-K)
Material Damping Ratio		N/A

Figure 25: Material properties of Copper in Solidworks.

K OF and Constraint Menu

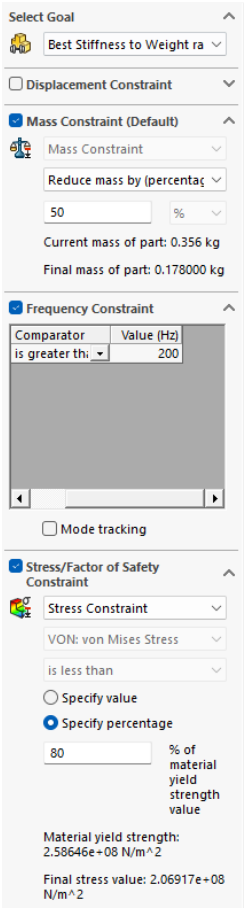

Figure 26: showing the objective function and constraint selection menu.

L Preserved Region Menu

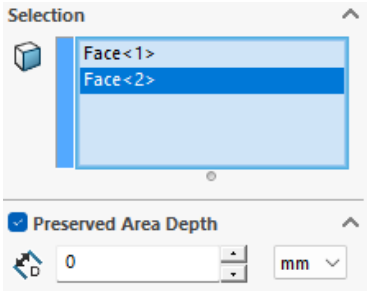

Figure 27: showing the preserved region menu with the DA and TS selected.

M Mass Slider Menu

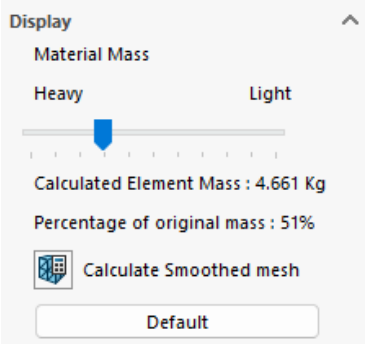

Figure 28: showing the mass slider menu and its default position.

N COMSOL Material Properties

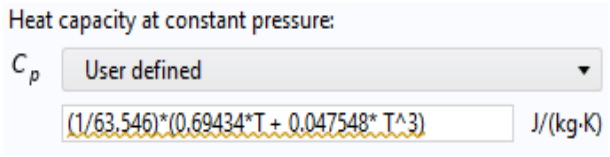

(a) Heat capacity definition menu.

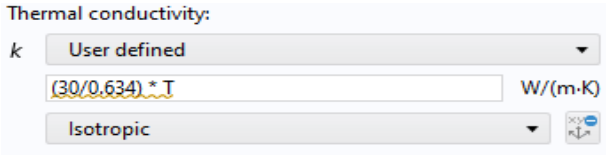

(b) Thermal conductivity definition menu.

Figure 29: showing the menus and corresponding equations for the material heat capacity and thermal conductivity.

O Baseline FPA Data

Table 6: COMSOL

Quantity	Mass[kg]	Avg. Temp. DA [mK]	Frequency [Hz]	max. vM stress [MPa]	m_0/m	k/k_0	C/10^-4
Value	9	0.050003	1948.2	103	1	1	0.4041309

Table 7: Solidworks

Quantity	Mass[kg]	Avg. Temp. DA [mK]	Frequency [Hz]	max. vM stress [MPa]	m_0/m	k/k_0	C/10^-4
Value	9	50.0	2033.9	63.17	1	1	0.4041309